

1 Article, Discoveries

2 **Flor yeasts rewire the central carbon metabolism during wine alcoholic**  
3 **fermentation.**

4 Emilien Peltier<sup>1,2,3</sup>, Charlotte Vion<sup>1,2</sup>, Omar Abou Saada<sup>3</sup>, Anne Friedrich<sup>3</sup>, Joseph Schacherer<sup>3,4</sup>,  
5 Philippe Marullo<sup>1,2</sup>

6

7 <sup>1</sup>University of Bordeaux, ISVV, Unité de recherche OEnologie EA 4577, USC 1366 INRA,  
8 33140 Bordeaux INP, Villenave d'Ornon, France

9 <sup>2</sup>Biolaffort, 33100 Bordeaux, France

10 <sup>3</sup>Université de Strasbourg, CNRS, GMGM UMR 7156, Strasbourg, France

11 <sup>4</sup>Institut Universitaire de France (IUF)

12

13 Corresponding author:

14 Emilien Peltier, GMGM,

15 IPCB

16 4 allée Konrad Roentgen, 67000 Strasbourg, France

17 [epeltier@unistra.fr](mailto:epeltier@unistra.fr)

18

## 19 **Abstract**

20 The identification of natural allelic variations controlling quantitative traits could contribute to  
21 decipher metabolic adaptation mechanisms within different populations of the same species.  
22 Such variations could result from man-mediated selection pressures and participate to the  
23 domestication. In this study, the genetic causes of the phenotypic variability of the central  
24 carbon metabolism *Saccharomyces cerevisiae* were investigated in the context of the enological  
25 fermentation. Carbon dioxide and glycerol production as well as malic acid consumption  
26 modulate the fermentation yield revealing a high level of genetic complexity. Their genetic  
27 determinism was found out by a multi environment QTL mapping approach allowing the  
28 identification of 14 quantitative trait loci from which 8 of them were validated down to the gene  
29 level by genetic engineering. Most of the validated genes had allelic variations involving flor  
30 yeast specific alleles. Those alleles were brought in the offspring by one parental strain that is  
31 closely related to the flor yeast genetic group while the second parental strain is part of the wine  
32 group. The causative genes identified are functionally linked to quantitative proteomic  
33 variations that would explain divergent metabolic features of wine and flor yeasts involving the  
34 tricarboxylic acid cycle (TCA), the glyoxylate shunt and the homeostasis of proton and redox  
35 cofactors. Overall, this work led to the identification of genetic factors that are hallmarks of  
36 adaptive divergence between flor yeast and wine yeast in the wine biotope. These alleles can  
37 also be used in the context of yeast selection to improve oenological traits linked to fermentation  
38 yield.

## 39 Introduction

40 Deciphering how the considerable phenotypic diversity observed at the species level is  
41 controlled by genetic variation is an important and non-trivial goal in biology. Improving  
42 knowledge regarding genotype-phenotype relationship provides information on evolution and  
43 adaptation mechanisms (Olson-Manning, Wagner, and Mitchell-Olds 2012) and is precious in  
44 many biological fields like medicine (Minikel et al. 2020) or food industry (McCouch 2004;  
45 Marullo et al. 2006; Sharmaa et al. 2015). Unravelling the genetic basis of adaptation highlights  
46 how organisms adapt to new selection pressure like climate change, new pathogens or drugs  
47 and vaccines (Olson-Manning, Wagner, and Mitchell-Olds 2012; Alföldi and Lindblad-Toh  
48 2013). Domestication is a specific case of adaptation with important phenotypic change  
49 emerging from human artificial selection. Domesticated organisms are a great opportunity to  
50 study adaptation as there is a better knowledge of their adaptive history through their well-  
51 characterized phenotypic properties and selective environments (Ross-Ibarra, Morrell, and Gaut  
52 2007; Gladieux et al. 2014). The identification of genes and molecular mechanisms leading to  
53 adaptation against domestication is also very useful in genetic selection in order to improve  
54 traits of economic interest and bringing phenotypic novelty to domesticated species (McCouch  
55 2004).

56 The yeast *Saccharomyces cerevisiae* rapidly emerged as an excellent model to study genotype-  
57 phenotype relationship (Steinmetz et al. 2002; Brem et al. 2002) and plenty of quantitative  
58 genetic studies were carried out in this species to study epistasis (Sinha et al. 2006), missing  
59 heritability (Bloom et al. 2013), gene-environment interaction (Smith and Kruglyak 2008;  
60 Bhatia et al. 2014; Yadav, Dhole, and Sinha 2016; Peltier et al. 2018) or impact of rare variants  
61 (Fournier et al. 2019; Bloom et al. 2019). *S. cerevisiae* was subjected to multiple domestication  
62 events in association with a large number of human associated environments (wine, beer, bread  
63 etc.) leading to distinct phylogenetic groups (Peter et al. 2018; Sicard and Legras 2011; J. L.  
64 Legras et al. 2018). Several genetic marks of adaptation were identified such as gene loss of  
65 function (Will et al. 2010), translocations (Zimmer et al. 2014; Pérez-Ortín et al. 2002),  
66 introgressions (Novo et al. 2009; Marsit et al. 2015), and SNPs (Peltier et al. 2019) (see for  
67 review : (Giannakou, Cotterrell, and Delneri 2020). Flor and wine yeasts are both associated  
68 with wine making environment and form two distinct but closely related phylogenetic groups  
69 (J. L. Legras et al. 2018). While both groups are able to efficiently perform wine fermentation,  
70 flor yeasts used in Sherry-like wines have the specific ability to shift to oxidative metabolism

71 and form a velum covering wine surface after fermentation (J. Legras et al. 2016). Differences  
72 in genomic content between wine and flor yeast were observed and the impact of allelic  
73 variations involved in biofilm formation were proposed as a feature of genetic adaptation  
74 (Fidalgo et al. 2006; Coi et al. 2017). Other functional adaptation hallmarks related to active  
75 gluconeogenesis, response to osmotic pressure and metal transport were predicted by a  
76 population genomic approach but have not been demonstrated yet at the gene level (Coi et al.  
77 2017).

78 Recent global warming caused the steady increase of sugar content in grape juices leading to  
79 higher ethanol concentration in wine with several issues regarding consumer health and wine  
80 quality (Dariusz R. Kutyna et al. 2010). Therefore, there is a growing demand for the  
81 development of new technologies to reduce alcohol content in wine. In this context, several  
82 institutions have attempted a biological approach in order to select new strains of *S. cerevisiae*  
83 with a lower fermentation yield. Various strategies were implemented such as adaptive  
84 evolution (Tilloy et al. 2015; D. R. Kutyna et al. 2012), interspecific breeding (da Silva et al.  
85 2015), and genetic engineering (Rossouw et al. 2013; Ehsani et al. 2009). Here, we aim at  
86 finding out undescribed natural genetic variations controlling the central carbon metabolism in  
87 order to modulate the efficiency of sugar into ethanol conversion (Fermentation yield). By  
88 applying a Quantitative Trait Loci (QTL) mapping approach, we investigated the genetic  
89 determinism of three traits (glycerol production, CO<sub>2</sub> production and malic acid consumption)  
90 that shape the carbon balance in enological conditions.

91 Our study is based on the analysis of a progeny obtained by crossing two strains derived from  
92 wine starters. A deeper analysis of parental genomes showed that, unexpectedly, one of the  
93 parental strains results to have a mosaic genome inherited from both wine and flor yeasts while  
94 the second parental strain belongs to the wine group. This admixture has promoted an important  
95 phenotypic variability impacting the central carbon metabolism of the F1 progeny. A total of  
96 14 QTLs were identified and the effect of eight of them were experimentally validated down to  
97 the gene level. Six genes (*PMA1*, *PNC1*, *PYC2*, *SDH2*, *MAE1*, and *MSB2*), among which three  
98 are directly involved in central carbon metabolism (*SDH2* in tricarboxylic acid cycle (TCA)),  
99 *MAE1* in pyruvate metabolism and *PYC2* in gluconeogenesis pathways, show allelic variations  
100 highly specific to flor yeasts group. Linked to these validated genes, further proteomic analyses  
101 highlighted different metabolic regulations between the parental strains for TCA and glyoxylate  
102 shunt. Altogether, these results support the hypothesis that allelic variations between wine and

103 flor yeasts generate important phenotypic differences and could be considered as hallmarks of  
104 adaptation for different growth strategies on the wine biotope. These results also show that flor  
105 yeasts constitute a great reservoir of genetic variation to bring phenotypic novelty in  
106 commercial yeast starter to cope for new challenges as global warming (Mira de Orduña 2010)  
107 and new viticultural practices (Kontoudakis et al. 2011).

## 108 **Results**

### 109 **Biometric study of the glycerol, CO<sub>2</sub> and malic acid**

110 In order to explore the genetic determinism of central carbon metabolism during wine alcoholic  
111 fermentation, the previous dataset of fermentation traits measured within a QTL mapping  
112 population was used (Peltier, Sharma, et al. 2018). This population was obtained by mating two  
113 fully homozygous strains (SB and GN) derived from the sporulation of wine starters. A total of  
114 94 meiotic segregants were obtained through sporulation of a single hybrid (SBxGN) (Fig1) and  
115 phenotyped in three environmental conditions using a small-scale fermentation dispositive and  
116 enzymatic assays to measure fermentation kinetics traits and endpoint concentration of several  
117 metabolites, including glycerol and CO<sub>2</sub> production. All segregants were sequenced and a  
118 genetic map of 3433 biallelic markers was built in order to identify the genetic factors  
119 controlling these phenotypes (Table S1). In the present study, an additional phenotyping effort  
120 was achieved by measuring malic acid consumption in the same conditions.

121

122 Carbon balance was evaluated by measuring the main organic compounds assimilated and/or  
123 produced for each of the 94 segregants at the end of the alcoholic fermentation (Table S2).  
124 According to the must, the fermentation yield computed ranged between 0.45 and 0.48 which  
125 is close to values observed in other studies (Tilloy, Ortiz-Julien, and Dequin 2014)  
126 (Supplementary file S1). An analysis of variance demonstrated a significant genetic (strain)  
127 impact on the fermentation yield (17% of the total variance explained). This integrative trait is  
128 mostly shaped by the quantitative variation of three metabolites: glycerol, malic acid, and CO<sub>2</sub>  
129 that were partially correlated (Figure S1). Glycerol and CO<sub>2</sub> (which is stoichiometrically linked  
130 to ethanol) are *de novo* synthesized by yeast catabolism; their concentrations are expressed in  
131 g/L. The final concentration of CO<sub>2</sub> produced is expressed hereafter as *CO<sub>2</sub>max*. The final  
132 concentration of malic acid depends on its initial amount in grape must which differs according

133 to the grape juice. Since this organic acid is partially metabolized by yeast, the strain  
134 contribution was normalized by computing the percentage of Malic Acid Consumed (*MAC%*).  
135 For each trait, parental strains SB and GN are significantly different with important gaps for  
136 glycerol and *MAC%* (Wilcoxon test,  $p$ val <0.05). Indeed, SB produces 1.6 g/L more glycerol  
137 (+30%) and consumes 28% more malic acid than GN. Since malic consumption and glycerol  
138 production have an opposite effect on CO<sub>2</sub> and ethanol production, the phenotypic differences  
139 for CO<sub>2</sub> are sharper. These differences are consistent with previous results showing that SB is  
140 the top strain for glycerol production and malic acid consumption compared to a panel of  
141 commercial starters (Peltier, Bernard, et al. 2018).

142 Each trait had a high overall heritability (Table S3) and displayed a bell-shaped distribution  
143 with number of segregants showing transgressive values respect to parental strains (Fig S2).  
144 These broad biometric observations highlighted a polygenetic control of each trait with a  
145 positive contribution of both parental strains.

#### 146 **Linkage analysis brings out a linkage hotspot with pleiotropic effect**

147 In a previous work that explored QTL interaction with environment, five QTLs were associated  
148 with *CO<sub>2</sub>max* and *glycerol* production in the SBxGN offspring (Peltier *et al.*, 2018). Here, we  
149 aimed at identifying supplemental QTL controlling *MAC%* that was newly phenotyped. A  
150 linkage analysis was performed and significantly associated nine QTLs to this trait. Therefore,  
151 a total of 14 QTL are involved in *CO<sub>2</sub>max*, *glycerol* and *MAC%* (Fig 2 and Table S4). The  
152 effects of parental alleles are shown in the Fig S3. Intriguingly, a large region of the  
153 chromosome VII (387 kb to 716 kb) was associated with all the considered traits. This linkage  
154 hotspot is almost entirely above the significance threshold for at least one trait and four distinct  
155 linkage peaks can be distinguished. This hotspot encompasses one major QTL, the locus  
156 *VII\_415* (Chr VII, position 415,719), influencing the glycerol production (LOD score >10)  
157 which explains more than 10 % of total variance. Interestingly, for this cross, a sharper region  
158 of chromosome VII (50 kb) was previously associated with kinetic traits during second  
159 fermentation of sparkling wines (Martí-Raga et al. 2017). Three genes of this large QTL (*PDR1*,  
160 *PMA1* and *MSB2*) were demonstrated to have an important phenotypic impact in this condition.  
161 Here, the QTL *VII\_482* linked to *MAC%* is located in the *PMA1* coding sequence (479,910  
162 482,666).

163 **Multiple Quantitative Trait Genes control glycerol production and malic acid**  
164 **consumption.**

165 Candidate genes neighboring the QTL peak within a 20 kb window were considered through  
166 their functional annotation and by checking for ns-SNPs within parental strains sequences using  
167 the algorithm SnpEff (Table S5) (Sherman and Salzberg 2020). We selected also the three genes  
168 (*PDR1*, *PMA1* and *MSB2*) previously validated for second fermentation traits that are located  
169 near the major hotspot of chromosome VII in the present work. This leads to consider 11  
170 candidate genes that could impact the traits investigated. Their effects were interrogated by a  
171 Reciprocal Hemizyosity Analysis (RHA) (Steinmetz et al. 2002). The impact of parental  
172 alleles was compared in alcoholic fermentation test using the same fermentation protocol. In  
173 addition, ethanol content (% Vol) was estimated by infrared reflectance rather than enzymatic  
174 assay (see methods). The effect of four candidate genes impacting *CO<sub>2</sub>max* and/or *glycerol* was  
175 tested. They belong to the two major QTLs found in term of variance explained: *ADE6*  
176 (*VII\_616*), *MSB2* (*VII\_512*), *PDR1* (*VII\_482*), *PNC1* (*VII\_415*). The RHA was carried out in  
177 the M15\_sk condition with two sugar concentration levels (219 and 265 g/L) using at least five  
178 biological replicates for each condition. Sugar spiking would emphasize the phenotypic  
179 differences related to CO<sub>2</sub> and ethanol production. The most obvious effects were obtained for  
180 glycerol production for genes *ADE6*, *MSB2*, and *PCNI* for which hemizygous hybrids are  
181 significantly different (Wilcoxon test, pval < 0.1) (Fig 3, panel A). These three genes are located  
182 in a region of 200 kb along the chromosome VII hotspot demonstrating that distinct genetic  
183 factors in this region control the glycerol production.

184 Intriguingly, the sugar content modulated the phenotypic responses of hemizygous hybrids.  
185 Indeed, in sugar-spiked grape must (M15\_265), alleles *ADE6<sup>GN</sup>* enhanced glycerol production  
186 of 12 %, while the allele *MSB2<sup>GN</sup>* has an enhancer effect only in the original M15 grape must  
187 (219g/L of initial sugar). The allelic forms *ADE6<sup>GN</sup>*, *PNC1<sup>SB</sup>* promote the glycerol production  
188 and their effects are those observed in the SBxGN progeny (Table S4, Fig S3). In contrast, the  
189 *MSB2<sup>GN</sup>* allele produced more glycerol which is not observed in the segregating progeny (Fig  
190 S4). This opposite effect has been previously described for the same gene for another phenotype  
191 and could be due to the complex genetic architecture of chromosome VII (Martí-Raga et al.  
192 2017). The difference observed in glycerol production for *ADE6*, *PNC1* and *MSB2* did not  
193 impact either the *CO<sub>2</sub>max* or the ethanol content.

194 In the same way, seven candidate genes belonging to six QTLs affecting *MAC%* were  
195 evaluated: *MAE1* (*XI\_381*), *MCH1* and *GPM2* (*IV\_356*), *PYC2* (*II\_669*), *PMA1* (*VII\_482*),  
196 *SDH2* (*XII\_53*) and *YBL036c* (*II\_152*). Fermentations were carried out in both M15 and SB14.  
197 RHA revealed a significant effect for the genes *MAE1*, *PMA1*, *PYC2* and *YBL036c* (Fig 3, panel  
198 B) (Wilcoxon test,  $pval < 0.05$ ). The alleles of *MAE1*, *PYC2* and *YBL036c* inherited from the  
199 parental strain SB consumed respectively 25%, 19%, and 45% more malic acid than those  
200 inherited from GN. In contrast, the *PMA1*<sup>GN</sup> allele consumed 18% more malic acid than  
201 *PMA1*<sup>SB</sup>. This gene, encoding for the plasma membrane ATPase, has been previously linked to  
202 the maintenance of pH homeostasis during wine fermentation and is located in the center of  
203 chromosome VII hotspot (Martí-Raga et al. 2017). Unexpectedly, a significant effect of *PNC1*  
204 on *MAC%* was also observed and the hemizygote hybrid harboring the *PNC1*<sup>SB</sup> allele consumes  
205 15 % more malic acid than *PNC1*<sup>GN</sup> (Fig 3, panel B) (Wilcoxon test,  $pval < 0.05$ ). The genomic  
206 position of *PNC1* is about 50 kb from the nearest QTL peak for *MAC%* *VII\_482*), however the  
207 other causative genes (*PMA1*, *MSB2*, *ADE6*) associated with the chromosome VII hotspot may  
208 have altered the precision of our linkage analysis.

209 Beside the validation of these five genes on *MAC%*, reciprocal hemizygous analysis of *SDH2*  
210 suggested its potential contribution on malic acid consumption. Although the hemizygous are  
211 not statistically different, a strong haploinsufficiency effect in both hemizygous hybrids was  
212 observed affecting either *MAC%* (-14%) and fermentation kinetics by doubling the  
213 fermentation duration (Fig S5). Intriguingly, this haploinsufficiency was only present in M15  
214 grape juice. Two factors suspected to have an impact on this haploinsufficiency were tested  
215 (initial malic concentration and pH) in synthetic grape juice (SGJ) by adjusting these two initial  
216 values to either M15 or SB14 levels. An haploinsufficiency similar to that in M15 was found  
217 in all four conditions even in the one mimicking SB14 conditions (Fig S5). No significant  
218 interaction between the level of haploinsufficiency and pH and malic acid was found (Anova,  
219  $pval > 0.1$ ). These findings suggest that *SDH2* has a great impact on fermentation rate and  
220 *MAC%* during grape juice fermentation. However, since the RHA test was limited by the  
221 haploinsufficiency effect our experiments failed to clearly demonstrate the impact of parental  
222 allelic variations.

223

224 Altogether, these functional analyses validated the role of eight Quantitative Trait Gene (QTG).  
225 Four of them play a direct role in the central metabolism encoding enzymes involved in



226 oxidoreductive reactions of carbohydrate metabolism (*MAE1*, *PYC2*, *PNC1*, *SDH2*). Two  
227 others are key regulators of osmotic (*MSB2*) and pH (*PMA1*) homeostasis. The RHA also  
228 revealed that *ADE6* and *YBL036c* contribute to the phenotypic difference between the parental  
229 strains for glycerol production and malic acid consumption, respectively (Fig 3). However, their  
230 functional connection with the metabolic pathway of glycerol and malic acid is more difficult  
231 to address at this stage.

## 232 **SB is a mosaic strain derived from flor and wine yeasts**

233 QTL mapping is a useful strategy for identifying natural genetic variations that shape  
234 phenotypic diversity between two strains. However, in most of the cases, the causative  
235 mutations identified are rare and specific to one parental strain (Bloom et al. 2019; Fournier et  
236 al. 2019; Peltier et al. 2019) due to the clonal structure of *S. cerevisiae* population (Peter et al.  
237 2018). This impairs the identification of more general mechanisms of adaptation resulting to  
238 natural selection. In order to have a more precise idea of the evolutive relevance of QTL  
239 identified, SB and GN genomes were compared to those of 403 wine related strains previously  
240 released (Peter et al. 2018; Legras et al. 2018). A phylogenetic tree was generated using 385,678  
241 SNPs discriminating the 403 wine strains plus the parental strains SB and GN. This collection  
242 of strains encompasses wine (n=358) and flor (n=47) strains that form distinct groups as  
243 previously described (Coi et al. 2017; Legras et al. 2018) (Table S6). Interestingly, SB is  
244 genetically close to the flor group while GN is quite similar to the wine group (Fig 4, panel A).  
245 Consequently, the two parental strains used in this study are quite distant with a sequence  
246 divergence of 0.19 % (~22,000 SNPs). The relatedness of SB genome with the flor group was  
247 deeply investigated by selecting a subset of 5,086 SNPs highly specific to the flor yeast group.  
248 Those SNPs have a frequency difference higher than 90 % between flor and wine yeast groups.  
249 The strain SB harbors 44.3 % of flor yeast specific alleles while GN only has 1.7 % of them.  
250 Their distribution across the SB genome is not uniform (Fig 4, panel B). Indeed, long portions  
251 of chromosomes have inherited 100 % flor-specific alleles (Chr II) while other portions are  
252 totally exempt of them (Chr VIII). This analysis demonstrated that SB is a mosaic strain  
253 between wine yeast and flor yeast, a feature shared with some others wine starters (Coi *et al.*,  
254 2017).

255

256 Intriguingly, nine of the fourteen QTLs mapped are located in flor specific chromosomal  
257 portions. This is the case of a large stretch within chromosome VII encompassing four causative  
258 genes (*PNC1*, *MSB2*, *PMA1*, *ADE6*) that displays the genomic signature of flor yeasts. A similar  
259 observation can be made for chromosome II in which three QTLs were identified (Fig 4, panel  
260 B). During their domestication, flor yeasts accumulated numerous mutations leading to an  
261 adaptation to grow on wine surface (Coi et al. 2017). In order to narrow such natural genetic  
262 variations, we listed the pool of ns-SNP discriminating SB and GN in the sequence of causative  
263 genes. For those SNPs, allelic frequencies of flor and wine groups were computed (Table 1). In  
264 *ADE6*, ns-SNPs listed are scarcely found whatever the group. The low allelic frequency of such  
265 polymorphisms would reflect recent mutations which is a common feature of the *S. cerevisiae*  
266 population. In contrast, for the other genes *PMA1*, *PNC1*, *PYC2*, *SDH2*, *MAE1*, and *MSB2*, the  
267 SB alleles are highly specific to flor yeast group while GN alleles are specific to the wine group.  
268 Therefore, these flor-specific alleles would have promoted the wide phenotypic variability of  
269 carbon metabolism observed in SBxGN progeny and more broadly are explaining phenotypic  
270 differences between flor and wine yeasts.

### 271 **SB proteome reveals peculiar metabolic regulations functionally connected with** 272 **some causative genes.**

273 Flor yeasts are able to grow on the wine surface at the end of the alcoholic fermentation. By  
274 creating biofilm rafts, they are able to resist to high ethanol content in harsh conditions (Legras  
275 et al. 2016). For ensuring their development, they activate particular metabolic pathways (active  
276 neoglucogenesis and respiration metabolism) that are the opposite of those developed by wine  
277 yeasts during the alcoholic fermentation. Such metabolic differences have been previously  
278 reported at the metabolomic and the proteomic levels (Moreno-García, García-Martínez,  
279 Moreno, et al. 2015; Moreno-García, García-Martínez, Millán, et al. 2015; Alexandre 2013;  
280 David-Vaizant and Alexandre 2018). In order to have a broad overview of the metabolic  
281 peculiarities of the SB strain, we reanalyzed a proteomic dataset previously generated in our  
282 laboratory (Albertin, Marullo, et al., 2013; Blein-Nicolas et al., 2013, 2015). Data explored  
283 were obtained by quantifying the proteome of 25 *S. cerevisiae* strains, including SB and GN,  
284 during the fermentation of a sauvignon blanc grape juice by a shotgun proteomics approach.  
285 Samples were collected at mid-point in triplicate allowing the quantification of 1110 proteins  
286 commonly expressed (Table S7). A global Principal Component Analysis (PCA) demonstrates  
287 that SB is strongly discriminated by the two principal axes accounting for 34 % of the total

288 inertia suggesting an outlier protein abundance respect to 24 other strains (Fig. 5, panel A).  
289 Indeed, the Abundance Fold Change Ratio (AFCR) of SB and GN vs the 24 other strains were  
290 compared for each of the 1100 proteins quantified. SB displays a much distinct profile since  
291 12.9 % of its proteome reach a 2 folds change abundance ( $\log_2(\text{AFCR}) \pm 1.0$ ) while only 2.9 %  
292 of GN proteins reach this threshold (Fig S6). Thus, proteome variance of SB and GN are 0.504  
293 vs 0.143, respectively (variance F test, pvalue  $< 1.10^{-16}$ ). This analysis demonstrated that SB has  
294 a particular proteome compared to GN and even to other *S. cerevisiae* strains.

295

296 In order to analyze the origin of this discrepancy, we deeply compared SB and GN using the  
297 1264 proteins quantified in both strains (Table S7). This comparative analysis reveals a set of  
298 207 proteins with an AFCR higher than 2 (Table S8). Within this set, a significant enrichment  
299 was found for mitochondrial proteins which represent 33% of the pool ( $\chi^2$  test =  $2.10^{-5}$ ). We  
300 sought functional interactions between the eight causative genes identified and the set of 207  
301 differentially expressed proteins by performing a STRING analysis (Szklarczyk et al. 2019)  
302 (see methods). Three of the six interaction networks computed clearly linked four QTG with  
303 proteins differentially expressed (Fig 5, panel B). The main cluster, linked to the causative  
304 genes *PYC2* and *MAEI*, encompassed 31 proteins including many enzymes related to pyruvate  
305 and citrate metabolism (Mls1p, Leu9p, Ach1p, Mdh3p, Dld1p, Dld2p, Ald5p, Cyb2p, Cit1p,  
306 Cit2p). The fold change abundance of such proteins suggests the existence of differential  
307 metabolic regulations between SB and GN. For instance, three of the four *S. cerevisiae* enzymes  
308 (Dld1p, Dld2p and Cyb2p) involved in the lactate metabolism are at least 2.5 less abundant in  
309 SB. These proteins are supposed to be repressed by glucose and anaerobiosis and participate to  
310 the oxidation of lactate into pyruvate (Bekker-Kettern, 2016). Other proteins, belonging to the  
311 glyoxylate shunt and TCA, were differentially quantified (2-fold change ratio). Interestingly,  
312 the oxidative branch of TCA and the glyoxylate shunt (i.e. Mls1p, Dal7p, Cit1p, Cit2p, Aco2p)  
313 are broadly more abundant in SB while proteins participating to the reductive branch of TCA  
314 (i.e. Fum1p, Mdh1, Sdh2p) are more abundant in GN (Fig S7, panel A). These metabolic  
315 pathways are directly connected with two causative genes identified in this study *MAEI* and  
316 *PYC2* that controls *MAC%*. Strikingly, the cytosolic malate synthase Mls1p catalyzing the  
317 condensation of glyoxylate and acetyl CoA in L-malate is 7 folds more abundant in SB  
318 ( $\log_2(\text{AFCR}) > 2.8$ ) and would directly enhance its cytosolic pool of malic acid. These  
319 noteworthy variations of proteins abundance are not due to a singular contrast between SB and

320 GN proteomes but reflect a clear specificity of SB central metabolism regulation. Indeed, the  
321 AFCR computed between SB and the 24 other *S cerevisiae* strains (average value) is very  
322 similar to the AFCR of SB vs GN (Pearson cor. test  $<10^{-13}$ ) (Fig S7 panel B). This analysis  
323 suggests that the peculiar proteome of SB would be due to its unusual mosaic origin  
324 encompassing large stretches of flor yeast genome.

325

## 326 Discussion

### 327 The flor yeast origin of the parental strain SB is likely involved in the diversity of 328 carbon catabolism in the SBxGN progeny.

329 This work aimed to identify natural genetic variations that possibly modulate the catabolism of  
330 carbon sources during wine fermentation. From an applied point of view, this goal is  
331 particularly relevant for wine industry in order to cope with two main negative effects of global  
332 warming: (i) the rise of ethanol content and (ii) the reduction of the total acidity of wines. This  
333 general trend is due to the increasing concentration of sugars coupled with a drop of malic acid  
334 content in grape juices around the world (van Leeuwen and Darriet 2016). By applying a QTL  
335 mapping strategy, eight Quantitative Trait Genes (QTG) impacting the carbon balance during  
336 the wine fermentation were identified. Although, reciprocal hemizygoty assay fails to identify  
337 candidate genes that significantly decrease the final ethanol content of wine, this study allows  
338 the identification of natural allelic variations controlling two remarkable phenotypes: the  
339 glycerol production and the percentage of malic acid consumed (MAC%). The schematic  
340 relationships of their respective proteins in the yeast metabolism map are shown on Fig 6.

341 This study was carried out using two meiotic segregants (SB and GN) derived from commercial  
342 starters widely used in wine industry (Actiflore BO213 and Zymaflore VL1, Laffort, France).  
343 Such commercial starters have been selected in the past for their technological properties by  
344 sampling spontaneous wine fermentations (P Marullo, pers com). Unexpectedly, we find out  
345 that the SB genome has a mosaic structure inherited from two distinct groups of *S. cerevisiae*  
346 population: the wine and the flor yeasts (Peter et al. 2018). Around 40 % of the SB genome is  
347 flor specific suggesting that BO213, the parental strain of SB, would be an F1-hybrid resulting  
348 from the cross of a flor yeast and a wine yeast, as previously observed for others wine  
349 commercial strains related to the Champagne group (Coi et al. 2017).

350 Wine yeasts are adapted to a fast development on grape must in competition with numerous  
351 other species in a sugar rich environment and many natural allelic variations related to their  
352 adaptation to grape juice have been described in the past (Peltier et al. 2019). In contrast, flor  
353 yeasts are adapted to survive in wine, a sugar-depleted environment containing high ethanol  
354 degree and low oxygen. Thus, flor yeasts would have accumulated specific genetic variations  
355 for coping with this harsh environment. Many efforts have been made for identifying such  
356 adaptation signatures especially concerning the development of the flor velum. This biofilm-  
357 like growth is essential for reaching the wine surface and to get oxygen which is mandatory for  
358 catabolizing ethanol and producing energy (Legras et al. 2016). Allelic variations specific to  
359 flor yeasts have been detected by using comparative genomics and the role of two genes (*SFL1*  
360 and *RGA2*) participating in the regulation of *FLO11* has been demonstrated (Coi et al. 2017).  
361 In the SBxGN cross, wine and flor specific alleles segregate providing the opportunity to study  
362 the phenotypic impact of gene pools that have undergone parallel evolutionary routes with  
363 different selective pressures. Indeed, nine of the fourteen QTL identified are located in flor  
364 specific regions allowing the molecular validation of six genes (*PMA1*, *PNC1*, *PYC2*, *SDH2*,  
365 *MAE1*, and *MSB2*) characterized by flor specific alleles. This suggest that part of the allelic  
366 variations involved in the adaptive divergence between wine and flor yeast had been captured.

367 Functionally, these genes are involved in key pathways discriminating flor yeast and wine yeast  
368 metabolisms. First, *MSB2* encodes a signaling mucin protein acting as a stress or nutrient  
369 deprivation receptor (Cullen and Sprague 2012). Msb2p is associated with the transmembrane  
370 osmosensor Sho1p and transmits the signal to the downstream components of the monomeric  
371 G-proteins Rho involved in both filamentous growth (FG) and the high osmolarity glycerol  
372 (HOG) pathways (Tatebayashi et al. 2007). HOG pathway plays a key role for adaptation  
373 against high osmolarity levels by increasing the production of glycerol (Hohmann, 2009), the  
374 second more abundant metabolite of fermenting yeast after ethanol. The comparative analysis  
375 of *MSB2* sequence reveals a unique ns-SNP between the parental strains (Table 1). The SB  
376 allele *S529F* is specific to flor yeasts and lowers the glycerol production respect to the GN  
377 allele. The *MSB2*<sup>*S529F*</sup> allele has a predicted deleterious effect that would impact the signal  
378 transduction of both HOG and FG MAPK pathways. Such pathways share common  
379 components but are induced by different stimuli and provides specific responses (Pitoniak et al.  
380 2009). The essential Rho protein Cdc42p has been described to stimulate glycerol production  
381 by triggering the MAPK Hog1p (Hohmann, 2009). Cdc42p is threefold less abundant in SB

382 which is consistent with the hypothesis of a low Msb2p activity in this background. In contrast  
383 the non-essential GTPase Rho3p also involved in cell polarity is three times more abundant in  
384 SB. Interestingly, the abundance fold ratio of Rho3p and Cdc42p are specific to SB (compared  
385 to others *S cerevisiae* strains) and might be related to the filamentous growth specificities of  
386 flor yeast required for the velum formation.

387 A flor-specific allele was also found in the sequence of *PNC1* which encodes for a  
388 nicotinamidase that converts nicotinamide to nicotinic acid. Pnc1p, which is induced by the  
389 osmotic stress, restores redox balance by regenerating NAD<sup>+</sup> from nicotinamide via the NAD<sup>+</sup>  
390 salvage pathway (Effelsberg et al. 2015; Ghislain, Talla, and François 2002). RHA reveals that  
391 the allele *PNC1<sup>SB</sup>* enhances both the glycerol production and the MAC%. A direct functional  
392 link exists between *PNC1* and glycerol biosynthesis since this protein is co-imported in the  
393 peroxisome with Gpd1p, a major controlling enzyme of glycerol biosynthesis (Nevoigt and  
394 Stahl 1997). Under osmotic stress, their overexpression saturates the peroxisome importation  
395 system and therefore this protein became cytosolic and active (Effelsberg *et al.*, 2015). The role  
396 of Pnc1p in MAC% is more complex to explain and might be linked to the NAD<sup>+</sup>/NADH<sup>+</sup>  
397 homeostasis itself that is tightly controlled (Bakker et al. 2001). This organic acid can be  
398 oxidized in pyruvate (by the malic enzyme Mae1p) or in oxaloacetate (by malate  
399 dehydrogenases). Thus, an active malic acid consumption would increase the intracellular  
400 levels of NADH<sup>+</sup> requiring an increase of glycerol production for regenerating the NAD<sup>+</sup> pool.

401  
402 Another flor yeast specific allele impacting MAC% is *MAE1* that encodes for the mitochondrial  
403 malic enzyme that catalyzes the oxidative decarboxylation of malate to pyruvate (Boles, de  
404 Jong-Gubbels and Pronk, 1998) achieving the malo-ethanolic fermentation (Volschenk,  
405 Vuuren and Viljoen–Bloom, 2003). Interestingly, *MAE1* was also reported to influence the  
406 formation of higher alcohols, fusel acids, and acetate esters in another mapping population  
407 where the same SNP is segregating (*MAE1<sup>1605V</sup>*) (Eder *et al.*, 2018). These data suggest that this  
408 allelic variation would have pleiotropic consequences in an enological context, affecting the  
409 malic acid consumption as well as the biosynthesis of relevant wine volatile compounds.

410  
411 A second pleiotropic gene to be discussed is *PMA1* which encodes for a membrane ATPase the  
412 major regulator of cytoplasmic pH and plasma membrane potential. During wine fermentation,

413 pH has a great impact on intracellular malic acid diffusion and consumption (Salmon, 1987;  
414 Delcourt *et al.*, 1995; Saayman and Viljoen-Bloom, 2006). Indeed, malic acid charge is strongly  
415 dependent of the wine pH since the *pka1* of this diacid is 3.54. Bellow a pH value of 3.4, the  
416 entry of a malic acid molecule in the cytoplasm result to a net proton influx that must be pumped  
417 over for maintaining pH homoeostasis with an energy cost of 1 ATP per molecule. In the present  
418 work, the QTL VII\_482 related to *PMAI* has the strongest effect observed with a positive  
419 impact of the GN allele on malic acid consumption. Previously, we demonstrated that *PMAI*  
420 inheritance influences fermentation kinetics with a strong interaction with the pH of the  
421 medium. Indeed the GN and SB alleles increase the fermentation rate when the pH are 3.3 and  
422 2.8, respectively (Martí-Raga *et al.*, 2017). These fine grain gene-environment interactions  
423 might result from the consumption level of malic acid in relation with the pH of wine.

424 Two other genes with a direct connection with malic acid metabolism were shed on light. The  
425 gene *PYC2* involved in gluconeogenesis pathway encodes for a pyruvate carboxylase that  
426 converts pyruvate to oxaloacetate (Stucka *et al.*, 1991; Walker *et al.*, 1991). During  
427 fermentation, pyruvate carboxylase is the sole source of oxaloacetate playing an essential role  
428 in aspartate biosynthesis, TCA turnover, and malic acid biosynthesis (Huet *et al.*, 2000). Indeed,  
429 *PYC2* overexpression enhances malic acid production in a bioengineering context (Bauer *et al.*,  
430 1999). We hypothesized that the allelic variants of SB may have reduced the Pyc2p activity  
431 reducing the biosynthetic flux of malic acid from pyruvate. To cope with this reduction, a first  
432 metabolic alternative would be the *de novo* synthesis of malic acid from the glyoxylate shunt.  
433 This is consistent with the high abundance of the malate synthase (more than 7 folds) observed  
434 in SB respect to GN. A second metabolic alternative would be a strongest uptake from the  
435 external media which is the hallmark of the SB strain.

436 Finally, a surprising effect of *SDH2* deletion was observed. This gene encodes for a subunit of  
437 the succinate dehydrogenase complex (complex II) ensuring electron transfer from succinate to  
438 ubiquinone. This TCA cycle step is involved in the mitochondrial respiratory chain and is  
439 mostly inactive during the alcoholic fermentation (Camarasa, Grivet and Dequin, 2003) due to  
440 oxygen depletion and catabolic repression (Klein, Olsson and Nielsen, 1998; Kwast, Burke and  
441 Poyton, 1998). Indeed, under sake brewing conditions, the CO<sub>2</sub> production rate was not  
442 impacted in double mutants  $\Delta sdh1$ ,  $\Delta sdh2$  (Kubo, Takagi and Nakamori, 2000). These  
443 commonly admitted results contrasted with the strong haploinsufficiency effect of *SDH2*  
444 deletion observed for *MAC%* and fermentation kinetics in M15 medium (Fig S5). Although we

445 could not measure a significant difference between hemizygous hybrids, the strong  
446 haploinsufficiency observed suggests that the succinate dehydrogenase complex would play an  
447 unsuspected physiological role in this specific background. Interestingly STRING analysis  
448 reveals that five proteins functionally associated to *SDH2* are differentially synthesized between  
449 SB and GN. These proteins belong to the respiratory complexes II, III and IV. Thus, complex  
450 II (Sdh1p and Sdh2p) is less abundant in SB while proteins belonging to complex III (Qcr10p)  
451 and IV (Cox2p and Cox12p) are more abundant. Due to the functional importance of protein  
452 stoichiometry in such complexes, abundance change in few proteins would impact the residual  
453 activity of the respiratory chain. Therefore, the functional understanding of the succinate  
454 dehydrogenase complex during alcoholic fermentation will require further analyses that are not  
455 the purpose on the present paper.

456

457 Flor yeasts exhibit an active gluconeogenesis and respiration catabolism during velum  
458 development that impact their proteomics response (Legras et al. 2016; Alexandre 2013)  
459 (Moreno-García, García-Martínez, Moreno, et al. 2015). However, to our knowledge, a  
460 comparative proteomic study between flor and wine yeast was never achieved. Since the SB  
461 strain harbor 40% of the genomic signature of a flor yeast, we supposed that this strain could  
462 exhibit particular flor yeast features at the proteomic level. This prompted us to compare the  
463 fermentation proteome of SB with other *S. cerevisiae* strains including the parental strain GN  
464 used in this study. A large comparative proteomics study between strains of the same species  
465 carried out in our laboratory was reanalyzed for this purpose (Blein et al. 2015). The abundance  
466 of 1100 proteins commonly quantified in 25 *S. cerevisiae* strains clearly demonstrated that SB  
467 exhibit a peculiar proteomic regulation (Fig 5, panel A) during wine fermentation (Table S7).  
468 Strikingly most of the proteins differentially regulated between SB and GN are due to the  
469 specific proteomic patterns of SB discarding the fact that the SB vs GN proteomic variations  
470 would be due to the GN strain (Fig S6, panel B). Several proteins involved in pyruvate and  
471 gluconeogenesis were differentially quantified. Many of them have been previously described  
472 as specific signature of velum development (Moreno-García, García-Martínez, Moreno, et al.  
473 2015).

474 By implementing a STRING analysis, we attempted to retrace a functional link between the  
475 eight QTG identified and the proteomic variations observed between parental strains. This  
476 indirect analysis would bridge the gap between specific flor yeast variations and the overall



477 proteomic discrepancy of the SB strain. Three causative genes (*MSB2*, *SDH2* and *PYC2*)  
478 harboring flor specific alleles were functionally connected with three protein clusters (Fig 5,  
479 panel B). *PYC2* and *SDH2* are directly involved in central carbon metabolism playing an  
480 essential role in gluconeogenesis and respiration, respectively. The first controls the unique way  
481 for producing glucose from ethanol since the pyruvate kinase catalyzed an irreversible reaction  
482 (Pronk, Steensma, and Van Dijken 1996). The second belongs to the succinate dehydrogenase  
483 which is inactivated during the fermentation and that constitutes the first step of respiration  
484 chain (complex II) which is essential for producing energy in aerobic conditions. A contrasted  
485 regulation between the oxidative and reductive branch of TCA was observed in the strain SB  
486 (Fig S7A) promoting the idea that succinate dehydrogenase activity would participate to the  
487 regulation of TCA proteome. Although this hypothesis remains to be validated by further  
488 experiments, we hypothesized that the specific flor alleles *Sdh2*<sup>K158E</sup> and *Pyc2*<sup>Q373K</sup> carried by  
489 SB strain might impact the overall proteomic response of this strain by controlling key steps of  
490 gluconeogenesis and TCA cycle.

## 491 **Materials and Methods**

### 492 **Yeast strains and culture media**

493 All the strains used in this study belong to the yeast species *Saccharomyces cerevisiae*. SB and  
494 GN strains are monosporic clones derived from industrial wine starters, VL1 and Actiflore  
495 BO213, respectively. Generation of the SBxGN and segregant populations were described by  
496 (Peltier, Sharma, *et al.*, 2018). Briefly, F1-hybrids were obtained by manual crossing with  
497 micromanipulator. After sporulation on ACK (2 % potassium-acetate, 2% agar) media,  
498 monosporic clones were isolated by micromanipulation. Yeast was cultured at 30 °c in yeast  
499 YPD media (10 g/L yeast extract, 20 g/L peptone and 20 g/L glucose) and solidified with 2 %  
500 agar when required. The strains were stored long term in YPD with 50% of glycerol at – 80 °C.

501

### 502 **Phenotyping**

503 The two grape juices used, Merlot of vintage 2015 (M15) and Sauvignon Blanc of vintage 2014  
504 (SB14), were provided by Vignobles Ducourt (Ladaux, France) and stored at – 20 ° C. Before  
505 fermentation, grape juices were sterilized by membrane filtration (cellulose acetate 0.45 µm

506 Sartorius Stedim Biotech, Aubagne, France). Fermentations were carried out as previously  
507 described (Peltier, Bernard, et al. 2018). Briefly, fermentations were run at 24 °C in 10 mL  
508 screw vials (Fisher Scientific, Hampton, New Hampshire, USA) with 5 mL of grape must.  
509 Hypodermic needles (G 26–0.45 × 13 mm, Terumo, Shibuya, Tokyo, Japan) were inserted  
510 through the septum for CO<sub>2</sub> release. Two micro-oxygenation conditions were used by applying  
511 or not constant orbital shaking at 175 rpm during the overall fermentation. For this data, three  
512 fermentation conditions were used: SB14 with shaking (SB14\_Sk), M15 with shaking (M15\_Sk)  
513 and M15 without shaking (M15). Fermentation progress was estimated by regularly  
514 monitoring the weight loss caused by CO<sub>2</sub> release using a precision balance. The amount of  
515 CO<sub>2</sub> released over time was modeled by local polynomial regression fitting with the R-loess  
516 function setting the span parameter to 0.45. From this model  $CO_{2max}$  parameter was  
517 extracted: maximal amount of CO<sub>2</sub> released (g.L<sup>-1</sup>) and the end of the fermentation.  
518 Fermentation conditions were described by (Peltier, Sharma, et al. 2018). Glycerol and malic  
519 acid concentration were determined by enzymatic assay (Peltier et al. 2018) using K-GCROLGK  
520 and K-LMAL-116A enzymatic kits (Megazyme, Bray, Ireland), following the instructions of the  
521 manufacturer.

522

### 523 **Linkage analysis**

524 The QTL mapping analysis was performed with the R/qlt package (Broman et al. 2003) on the  
525 data collected in the three environmental conditions by using the Haley-Knott regression  
526 model that provides a fast approximation of standard interval mapping (Haley and Knott  
527 1992). The analysis is taking in account environment and cross as an additive covariate, aiming  
528 to identify QTL robust to environment and cross factor:

$$529 \quad y_i = \mu + \beta_{g_i} + A_Y + \epsilon$$

530 Where  $y_i$  is the phenotype for individual  $i$ ,  $\mu$  the average value,  $\beta_{g_i}$  the QTL genotype for  
531 individual  $i$ ,  $A_{YZ}$  the matrix of environment covariates ( $y = M15\_Sk, SB14\_Sk, M15$ ) and  $\epsilon$  the  
532 residual error. For each phenotype, a permutation test of 1000 permutations tested the  
533 significance of the LOD score obtained, and a 5% FDR threshold was fixed for determining the

534 presence of QTLs (Churchill and Doerge 1994). The QTL position was estimated as the marker  
535 position with the highest LOD score among all markers above the threshold in a 30 kb window.

### 536 **Hemizygous hybrids construction**

537 For each QTL, candidate genes were sought in a 30 kb windows around the QTL position with  
538 the maximal LOD score. Genes with non-synonymous SNPs and/or with a function related to  
539 the trait of interest were retained. Candidate genes were validated by reciprocal hemizyosity  
540 analysis according to (Steinmetz et al., 2002) using SBxGN hybrid. Deletion cassettes were  
541 obtained by PCR amplification of the disruption cassette plus 500 pb of the flanking regions  
542 using as genomic template the genomic DNA of the strains Y04691, Y03717, Y04878, Y03751,  
543 Y04405, Y01529, Y03062 of the EUROSCARF collection (<http://euroscarf.de>), which contain  
544 disruption cassettes for the following genes: *ADE6*, *GPM2*, *MAE1*, *MCH1*, *PNC1*, *PYC2*, *SDH2*,  
545 *YBL036C*, respectively. Primers used for strains construction are listed in File S2. Reciprocal  
546 hemizygotes for *MSB2*, *PDR1* and *PMA1* were previously constructed with the same strategy  
547 by (Martí-Raga et al., 2017).

### 548 **Phylogenetic analysis**

549 Publicly available sequences of yeasts from wine and flor genetic groups were retrieved from  
550 (Peter et al. 2018; Legras et al. 2018) and are listed in table S6. A matrix of 385,678 SNPs was  
551 generated with GenotypeGVCFs from GATK after gvcf files were constructed as detailed in  
552 (Peter et al. 2018). This matrix was used to build a neighbor-joining tree using the *ape* and  
553 *SNPrelate* R packages. Flor and wine yeast genetic groups were determined according to (Peter  
554 et al. 2018; Legras et al. 2018) and correspond to the flor genetic group and the Wine/European  
555 (subclade 4), respectively. Flor yeast specific alleles were defined as alleles with a frequency  
556 difference of 90 % between flor and wine genetic groups.

### 557 **Proteomic data reanalysis**

558 The dataset used for reanalyzing proteome specificities of the strain SB correspond to the  
559 supplementary *table S5* published by Blein et al. (2015). This dataset compassed the proteomes  
560 of 66 *Saccharomyces* strains quantified during the alcoholic fermentation of a Sauvignon blanc  
561 grape juice at two temperatures. Among those strains, 28 *S cerevisiae* strains constituting a half-  
562 diallel design of 7 parental strains of different origins and 21 F1-hybrids. In that study the

563 parental strains SB and GN were referenced as E2 and E3, respectively. A subset portion of this  
564 large data set was reanalyzed for narrowing down the proteomic specificities of the strain SB.  
565 Only the proteome corresponding to *S cerevisiae* strains measure at 26°C were kept. Indeed,  
566 proteomic data for the strain E2 (SB) at 18°C were not available. In addition, we removed the  
567 proteomes of the strains W1, EW21 and EW31 due to the lower number of proteins quantified  
568 (<900) respect to the other strains. By applying these filters, we analyzed the abundance of 1100  
569 proteins commonly quantified in 25 *S. cerevisiae* strains including GN and SB. In addition, the  
570 list of the 1264 proteins specifically detected between SB and GN was listed in the table S7.  
571 The abundance values indicated in are the average of three biological replicates where 90% of  
572 the data points have a CV% lower than 5.37. The Abundance Fold Change Ratio (AFCR) of  
573 the strains SB and GN were expressed in log<sub>2</sub> for an easier comparison. An arbitrary AFCR  
574 threshold of +/-1 was used for selected proteins having a relevant abundance change, this basic  
575 threshold is widely used in the proteomics literature. The table S8 provides the list of the 207  
576 proteins selected in the set of the 1264 proteins common to SB and GN. Proteins with a  
577 differential abundance between SB and GN were used for computing a STRING analysis in  
578 order to find out functional connections with the eight genes validated in this study. The  
579 permanent link of such analysis is the following [https://version-11-0.string-](https://version-11-0.string-db.org/cgi/network.pl?networkId=pEeVlh8dPgJJ)  
580 [db.org/cgi/network.pl?networkId=pEeVlh8dPgJJ](https://version-11-0.string-db.org/cgi/network.pl?networkId=pEeVlh8dPgJJ). The interaction classes interrogated were  
581 “experiments” and “databases” with the highest confidence score.

## 582 **Statistical analyses**

583 All the statistical and graphical analyses were carried out using R software (R Core Team 2018).

584 The *lato sensu* heritability  $h^2$  was estimated for each phenotype as follows:

$$585 \quad h^2 = \frac{\sigma P^2 - \sigma E^2}{\sigma P^2}$$

586 where  $\sigma P^2$  is the variance of progeny population in each environmental conditions, explaining  
587 both the genetic and environmental variance of the phenotype measured, whereas  $\sigma E^2$  is the  
588 median of the variance of replicates in each environmental conditions, explaining only the  
589 environmental fraction of phenotypic variance.

590

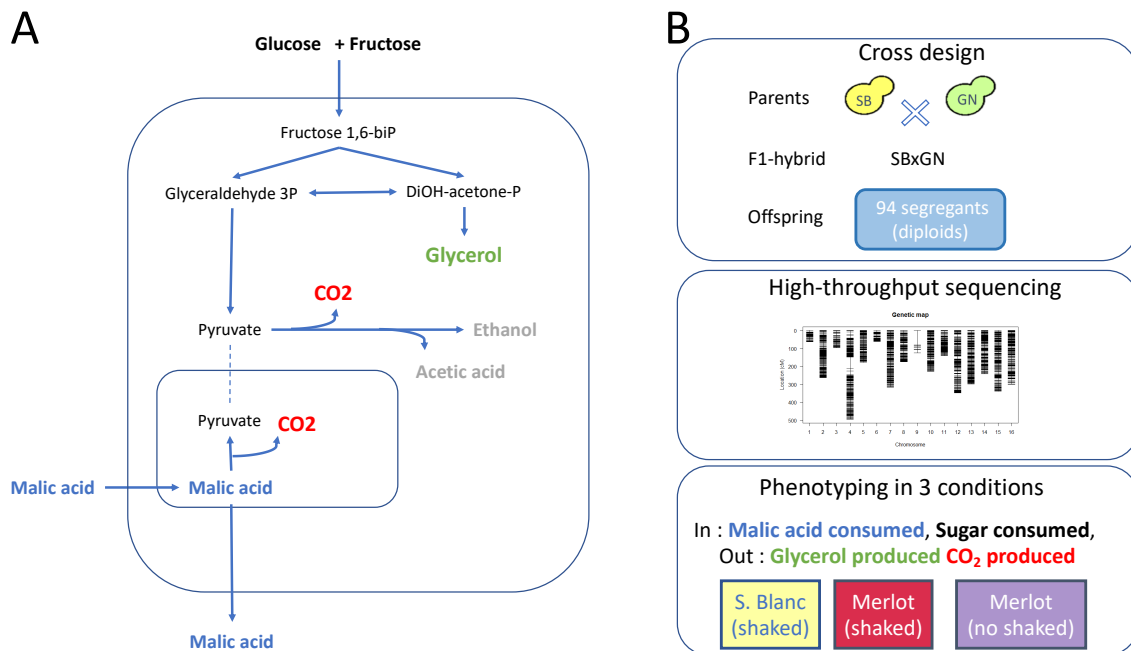
591 **Acknowledgements and funding information**

592 The authors thank Justine Pape, Dylan Dos Reis and Elodie Kaminski that helped managing  
593 fermentations. This work was funded by Région d'Aquitaine ([https://www.nouvelle-](https://www.nouvelle-aquitaine.fr)  
594 [aquitaine.fr](https://www.nouvelle-aquitaine.fr)). The funders had no role in study design, data collection and analysis, decision to  
595 publish, or preparation of the manuscript.

596

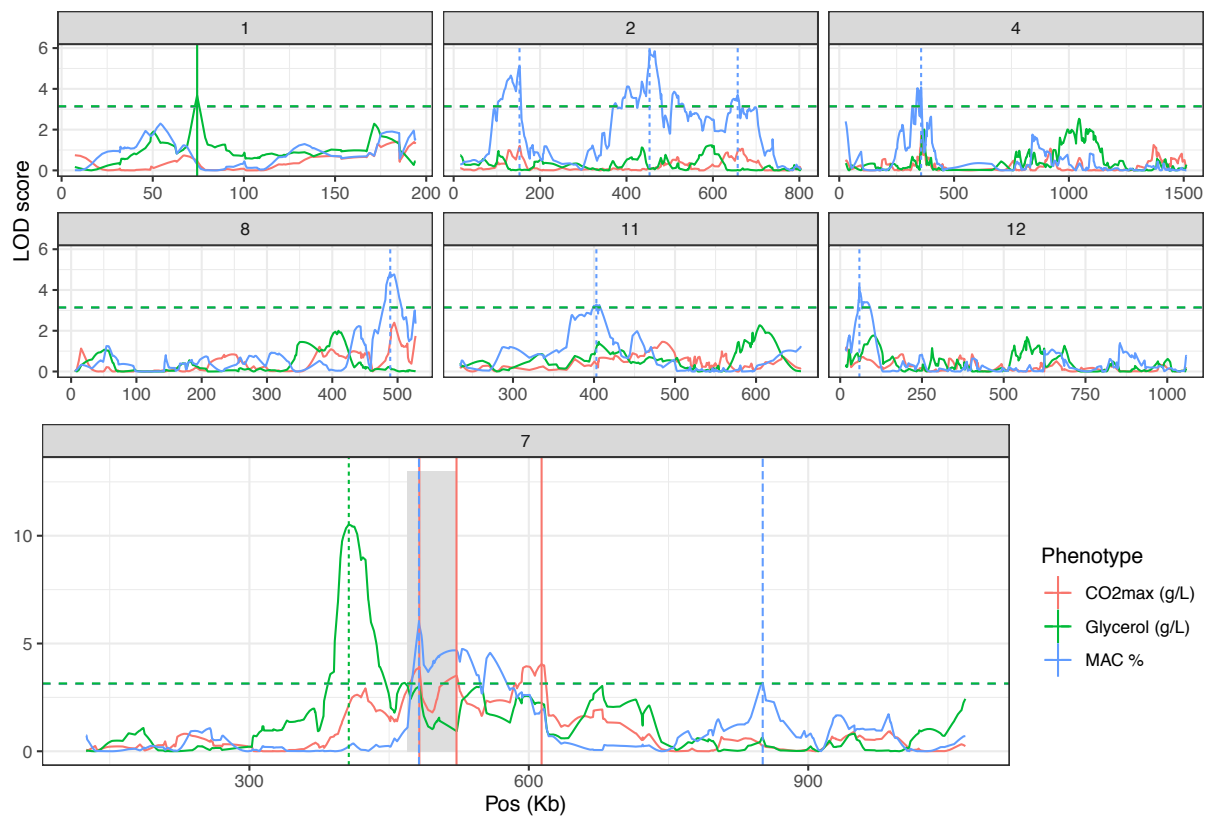
597 **Figure**

598 **Figure 1. Experimental design.**



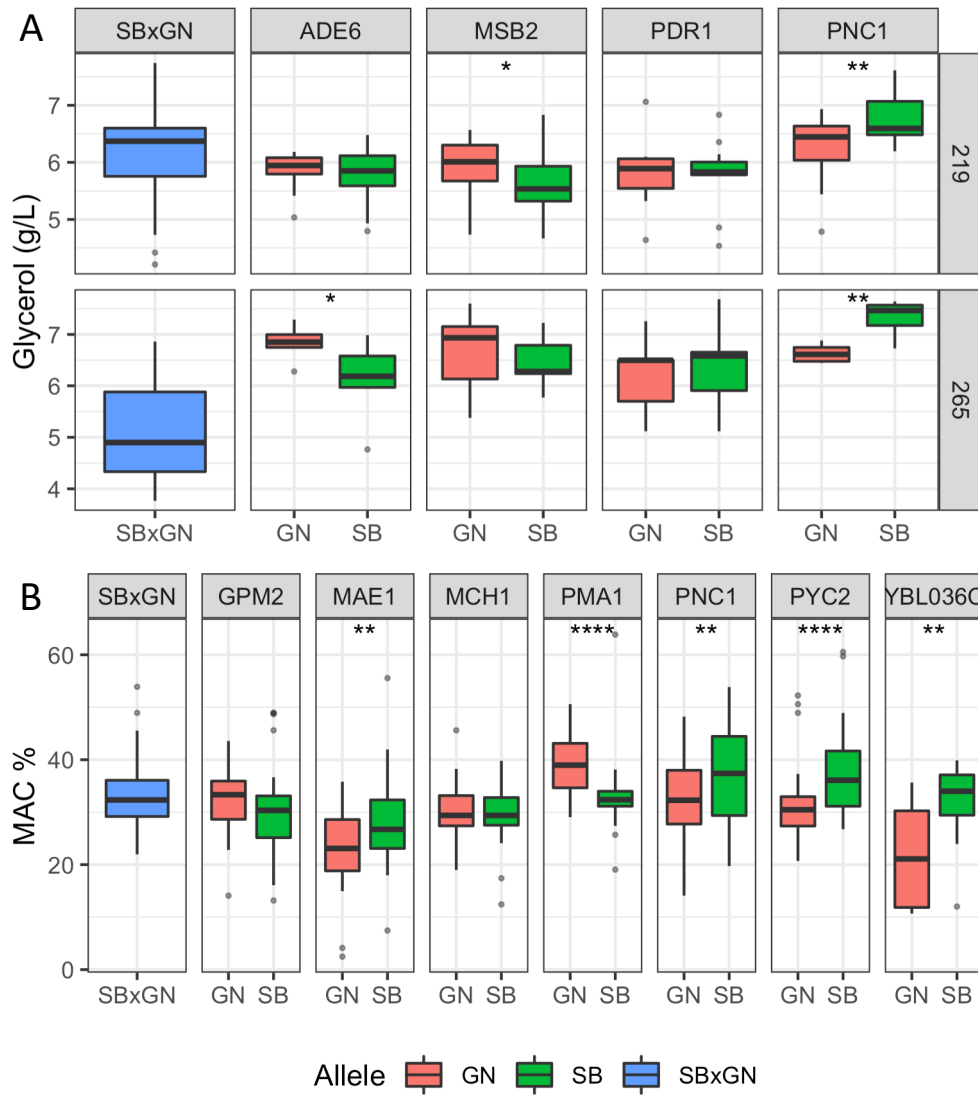
599

600 **Figure 2. Linkage analysis leads to the identification of 14 QTLs.**



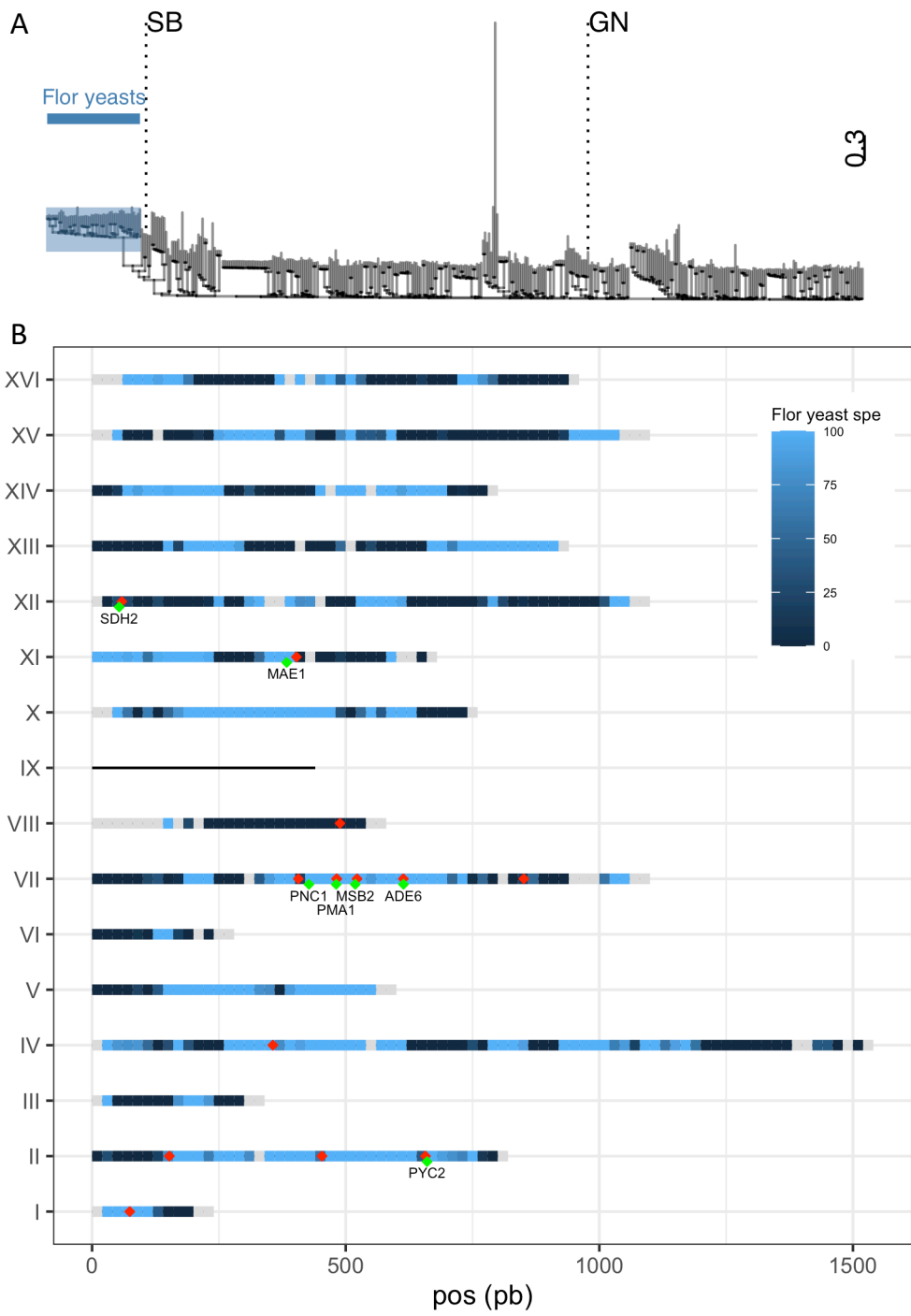
601

602 **Figure 3. Results of the reciprocal hemizyosity analysis**



603

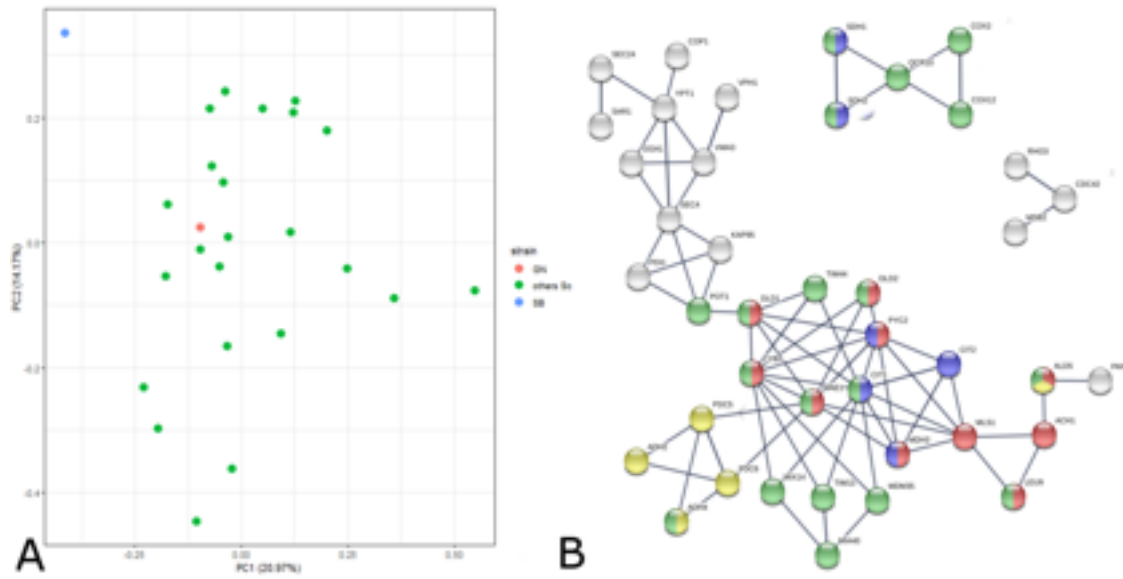
604 **Figure 4. SB is closely related to flor yeasts**



605

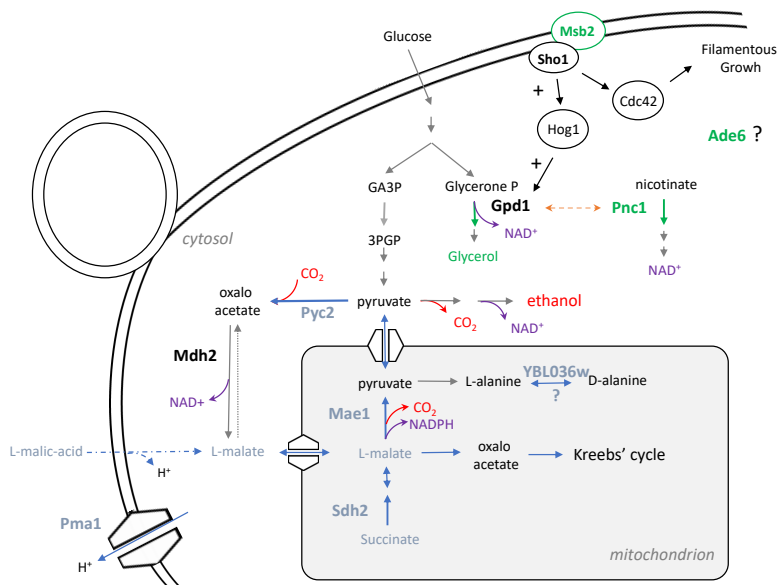


606 **Figure 5. Proteomic analysis reveals the outlier behavior of the SB strain**



607

608 **Figure 6. Relative position of the eight QTG in the metabolic map of *S cerevisiae***



609

## 610 **Figure Legends**

### 611 **Figure 1. Experimental design.**

612 **Panel A.** Overview of yeast central carbon metabolism during fermentation with the main  
613 carbon input and output. **Panel B.** Segregant population, genetic map and phenotypic  
614 conditions used for QTL mapping.

### 615 **Figure 2. Linkage analysis leads to the identification of 14 QTLs.**

616 Linkage analysis results for the *CO<sub>2</sub>max*, *Glycerol* and *MAC%* for chromosome with at least  
617 one QTL. Horizontal lines represent the threshold of significance according to permutation test  
618 (FDR = 5 %). Vertical lines highlight QTL peaks. Grey shadow encompasses the previously  
619 identified QTL hotspot containing *PDR1*, *MSB2* and *PMAI* (Martí-Raga *et al.*, 2017).

### 620 **Figure 3. Results of the reciprocal hemizyosity analysis**

621 Boxplot are colored according to the allele present in the hemizygous hybrids (blue = both, red  
622 = GN and green = SB) and represented the dispersion of at least five biological replicates. A  
623 Wilcoxon–Mann–Whitney test was applied to assess the significance of the phenotypic  
624 difference between hemizygotes. The level of significance is indicated as follows: \*  $p \leq 0.1$ , \*\*  
625  $p \leq 0.05$ , \*\*\*  $p \leq 0.01$  and  $p \leq 0.001$ \*\*\*\*. **Panel A.** RHA result for glycerol. **Panel B.** RHA  
626 result for *MAC%*.

### 627 **Figure 4. SB is closely related to flor yeasts**

628 **Panel A.** Dendrogram using 385,678 SNPs from 405 wine strains. Flor yeasts group is  
629 highlighted. **Panel B.** Percentage of specific allele own by SB along the genome is represented  
630 by a gradient from dark blue (0 %) to light blue (100 %). Grey portions represent genome tracks  
631 without any flor yeast specific allele. SB is aneuploid for chromosome IX and therefore is not  
632 considered in this analysis. The 20 QTLs mapped are shown with red dots (some of them are  
633 overlapping) and validated genes are shown in green.

### 634 **Figure 5. Proteomic analysis reveals the outlier behavior of the SB strain**

635 **Panel A.** We reanalyzed a proteomic dataset previously obtained by shotgun quantitative  
636 proteomics (Blein *et al.* 2015). Yeast samples of 25 *S. cerevisiae* strains including SB and GN)  
637 were collected at mid fermentation of a Sauvignon blanc grape juice. A set of 1110 proteins  
638 common to all the strain was selected for analyzing strain relationships by a principal

639 component analysis. The first two components representing 34% of the total inertia illustrate  
 640 that the proteome of the strain SB (blue point) is quite divergent from the other *S. cerevisiae*  
 641 strains including GN (red point). **Panel B** The functional interactions between 207 differentially  
 642 expressed proteins and the eight QTG validated in this study was interrogated by using STRING  
 643 algorithm. The three clusters encompassed 2, 4 and 31 proteins showing a strong functional  
 644 interaction with the four causative genes *PYC2*, *MAE1*, *MSB2* and *SDH2*, (black crosses).  
 645 Active interactions were computed using the STRING algorithm on the base of experimental  
 646 data and annotated database with a minimal interaction score of 0.8. Proteins were colored  
 647 according to their mitochondrial origin (red), their involvement in pyruvate metabolism (blue)  
 648 or in neo glucogenesis (green).

649 **Figure 6. Relative position of the eight QTG in the metabolic map of *S. cerevisiae***

650 The metabolic relationships between the eight causative genes identified in this study is  
 651 presented. Genes impacting glycerol production are represented in green while genes impacting  
 652 *MAC%* are presented in blue.

653 **Tables**

654 **Table 1. ns-SNPs in validated genes according to genetic group**

| ORF            | Gene        | Protein size | Trait impacted | ns-SNP         |             | Frequency in |            | deleterious effect <sup>a</sup> |
|----------------|-------------|--------------|----------------|----------------|-------------|--------------|------------|---------------------------------|
|                |             |              |                | Protein allele | Inheritance | wine group   | flor group |                                 |
| <i>YGR061C</i> | <i>ADE6</i> | 1359         | Glycerol       | F181L          | SB          | 1.7          | 12.8       | no                              |
|                |             |              |                | V570I          | SB          | 1.8          | 3.2        | no                              |
|                |             |              |                | P745S          | GN          | 0.4          | 0          | no                              |
|                |             |              |                | V1238A         | SB          | 2            | 4.3        | yes                             |
| <i>YGL008C</i> | <i>PMA1</i> | 919          | <i>MAC%</i>    | P74L           | GN          | 96.3         | 0          | yes                             |
|                |             |              |                | L176M          | SB          | 0.6          | 27.7       | no                              |
|                |             |              |                | D200E          | SB          | 0.6          | 10.6       | yes                             |
|                |             |              |                | E283R          | SB          | 2.7          | 100        | no                              |
|                |             |              |                | L290V          | SB          | 0.6          | 27.7       | no                              |
|                |             |              |                | K431I          | SB          | 0            | 0          | no                              |
|                |             |              |                | Q432E          | SB          | 0            | 0          | no                              |
|                |             |              |                | D718N          | SB          | 3.5          | 100        | no                              |
|                |             |              |                | E875Q          | SB          | 2.7          | 97.9       | yes                             |

|         |      |      |                |       |    |      |      |     |
|---------|------|------|----------------|-------|----|------|------|-----|
| YGL037C | PNC1 | 217  | Glycerol. MAC% | V112A | SB | 1.7  | 100  | no  |
| YBR218C | PYC2 | 1181 | MAC%           | Q373K | SB | 1.7  | 78.7 | no  |
|         |      |      |                | E722K | SB | 0.1  | 0    | no  |
| YLL041C | SDH2 | 267  | MAC%. kinetics | K158E | SB | 1.3  | 100  | no  |
| YGR014W | MSB2 | 1306 | Glycerol       | S529F | SB | 1.7  | 98.9 | yes |
| YKL029C | MAE1 | 669  | MAC%           | I605V | GN | 64.9 | 0    | no  |

655 a ns-SNP have been predicted to be to have a deleterious effect on protein according to  
656 PROVEAN algorithm

## 657 Supplementary Figure

### 658 Fig S1. Correlation between traits.

659 Correlation between traits. Data is normalized according to environment. Each dot represents  
660 the average value of an individual in one of the three phenotypic condition. Correlation  
661 coefficient and P value of Spearman's correlation test is indicated.  $CO_2max$  is negatively  
662 correlated with *glycerol* and positively correlated with *MAC%* (Spearman test,  $pval < 0.01$ ).  
663 However,  $\rho$  values observed are quite low ( $<0.2$ ) because the variation in  $CO_2$  production is  
664 balanced by glycerol production and malic acid consumption.

### 665 Fig S2. Distribution of traits.

666 **Left.** Distribution of the progeny according to trait and media is represented. Dashed vertical  
667 line represent parental average value. **Right.** Data is normalized according to environment.  
668 Distribution of the progeny in all media, according to trait and cross. Dashed vertical line  
669 represent parental average value.

### 670 Fig S3. QTL effect in population.

671 Effect of each QTL according to parental inheritance. Each dot represents the phenotypic value  
672 of one individual and are colored according to their marker inheritance. Bigger points  
673 represent the mean of the population.

### 674 Fig S4. Discrepancy for MSB2

675 **Panel A.** Effect of the marker associated to *MSB2* in the offspring. Each dot represents the  
676 phenotypic value of one individual and are colored according to their marker inheritance.

677 **Panel B.** Result of RHA test for *MSB2*. The represented value is from at least 5 biological  
678 replicates. The level of significance is indicated as follows: \*  $p \leq 0.1$ . \*\*  $p \leq 0.05$ . \*\*\*  $p \leq 0.01$ .  
679 Solid lines of kinetic curves represent the mean and the shadow the standard error.

680

681 **Fig S5. *SDH2* hemizygotes show a substantial haploinsufficiency according to**  
682 **media.**

683 The represented value is from at least 5 biological replicates. A Wilcoxon–Mann–Whitney test  
684 was applied to assess the significance of the phenotypic difference between wild type and  
685 hemizygote. The level of significance is indicated as follows: \*  $p \leq 0.1$ . \*\*  $p \leq 0.05$ . \*\*\*  $p \leq 0.01$ .  
686 Solid lines of kinetic curves represent the mean and the shadow the standard error.

687 **Fig S6. SB proteome exhibit a strongest variability than GN respect to 24 others *S***  
688 ***cerevisiae* proteomes.**

689 The plot represents the distribution of the Abundance Fold Change Ratio (expressed in  $\log_2$ ) of  
690 the strains SB and GN respect to the average values of 24 other strains. The variance of SB and  
691 GN computed for the 1110 proteins indicated a highest variability of the SB proteome (F-test  
692 analysis  $< 1.10^{-7}$ ).

693 **Fig S7. Abundance of proteins belonging to the oxidative and reductive branches**  
694 **of TCA in SB respect to GN and others *S cerevisiae* strains**

695 Panel A. Abundance fold ratio of quantified proteins belonging to the TCA and the glyoxylate  
696 shunt; red and green colors indicated over and under expressed proteins in the SB strain *vs* GN  
697 (left box) or *vs* the average value of 24 *S cerevisiae* strains (right box). Panel B. correlation  
698 between the AFRCR ( $\log_2$ ) of SB *vs* GN and SB *vs* 24 *S. cerevisiae* strains for the commonly  
699 expressed proteins.

## 700 **Supplementary file**

701 **File S1. Assessment of the alcoholic fermentation yield and variability of carbon**  
702 **use in wine fermentation**

703 **File S2. Hemizygotes construction**

704

705 **Supplementary tables**

706 **Table S1. Genotype data of offspring**

707 **Table S2. Phenotype data of offspring**

708 **Table S3. Heritability**

709 **Table S4. QTL list**

710 **Table S5. Candidate genes**

711 **Table S6. Strains used for phylogeny analysis**

712 **Table S7. Protein dataset**

713 **Table S8. Protein difference SB vs GN**

714 **Data Availability Statement**

715 **Phylogenic analysis**

716 **References**

717 Albertin, Warren, Philippe Marullo, Marina Bely, Michel Aigle, Aurélie Bourgeois, Olivier  
718 Langella, Thierry Balliau, et al. 2013. "Linking Post-Translational Modifications and  
719 Variation of Phenotypic Traits." *Molecular & Cellular Proteomics : MCP* 12 (3): 720–35.  
720 <https://doi.org/10.1074/mcp.M112.024349>.

721 Alexandre, Hervé. 2013. "Flor Yeasts of *Saccharomyces Cerevisiae*-Their Ecology, Genetics and  
722 Metabolism." *International Journal of Food Microbiology* 167 (2): 269–75.  
723 <https://doi.org/10.1016/j.ijfoodmicro.2013.08.021>.

724 Alföldi, Jessica, and Kerstin Lindblad-Toh. 2013. "Comparative Genomics as a Tool to  
725 Understand Evolution and Disease." *Genome Research*. *Genome Res.*  
726 <https://doi.org/10.1101/gr.157503.113>.

727 Bakker, Barbara M., Karin M. Overkamp, Antonius J a Van Maris, Peter Kötter, Marijke a H  
728 Luttik, Johannes P. Van Dijken, and Jack T. Pronk. 2001. "Stoichiometry and

- 729           Compartmentation of NADH Metabolism in *Saccharomyces Cerevisiae*.” *FEMS*  
730           *Microbiology Reviews* 25 (1): 15–37. [https://doi.org/10.1016/S0168-6445\(00\)00039-5](https://doi.org/10.1016/S0168-6445(00)00039-5).
- 731   Bauer, Jargen, Marijke A.H. Luttik, Carmen-Lisset Flores, Johannes P. Dijken, Jack T. Pronk,  
732           and Peter Niederberger. 1999. “By-Product Formation during Exposure of Respiring  
733           *Saccharomyces Cerevisiae* Cultures to Excess Glucose Is Not Caused by a Limited Capacity  
734           of Pyruvate Carboxylase.” *FEMS Microbiology Letters* 179 (1): 107–13.  
735           <https://doi.org/10.1111/j.1574-6968.1999.tb08715.x>.
- 736   Blein-Nicolas, Melisande, Warren Albertin, Telma da Silva, Benoıt Valot, Thierry Balliau,  
737           Isabelle Masneuf-Pomarede, Marina Bely, et al. 2015. “A Systems Approach to Elucidate  
738           Heterosis of Protein Abundances in Yeast.” *Molecular & Cellular Proteomics : MCP* 14 (8):  
739           2056–71. <https://doi.org/10.1074/mcp.M115.048058>.
- 740   Blein-Nicolas, Melisande, Warren Albertin, Benoıt Valot, Philippe Marullo, Delphine Sicard,  
741           Christophe Giraud, Sylvie Huet, et al. 2013. “Yeast Proteome Variations Reveal Different  
742           Adaptive Responses to Grape Must Fermentation.” *Molecular Biology and Evolution* 30  
743           (6): 1368–83. <https://doi.org/10.1093/molbev/mst050>.
- 744   Bloom, Joshua S., James Boocock, Sebastian Treusch, Meru J. Sadhu, Laura Day, Holly Oates-  
745           Barker, and Leonid Kruglyak. 2019. “Rare Variants Contribute Disproportionately to  
746           Quantitative Trait Variation in Yeast.” *ELife* 8 (October).  
747           <https://doi.org/10.7554/eLife.49212>.
- 748   Boles, E, P de Jong-Gubbels, and J T Pronk. 1998. “Identification and Characterization of MAE1,  
749           the *Saccharomyces Cerevisiae* Structural Gene Encoding Mitochondrial Malic Enzyme.”  
750           *Journal of Bacteriology* 180 (11): 2875–82.
- 751   Broman, Karl W., Hao Wu, aunak Sen, and Gary A. Churchill. 2003. “R/Qtl: QTL Mapping in  
752           Experimental Crosses.” *Bioinformatics* 19 (7): 889–90.  
753           <https://doi.org/10.1093/bioinformatics/btg112>.
- 754   Camarasa, Carole, Jean Philippe Grivet, and Sylvie Dequin. 2003. “Investigation by <sup>13</sup>C-NMR  
755           and Tricarboxylic Acid (TCA) Deletion Mutant Analysis of Pathways of Succinate  
756           Formation in *Saccharomyces Cerevisiae* during Anaerobic Fermentation.” *Microbiology*

757 149 (9): 2669–78. <https://doi.org/10.1099/mic.0.26007-0>.

758 Churchill, G. A., and R. W. Doerge. 1994. “Empirical Threshold Values for Quantitative Trait  
759 Mapping.” *Genetics* 138 (3): 963–71. <https://doi.org/10.1007/s11703-007-0022-y>.

760 Coi, A. L., F. Bigey, S. Mallet, S. Marsit, G. Zara, P. Gladieux, V. Galeote, M. Budroni, S. Dequin,  
761 and J. L. Legras. 2017. “Genomic Signatures of Adaptation to Wine Biological Ageing  
762 Conditions in Biofilm-Forming Flor Yeasts.” *Molecular Ecology* 26 (7): 2150–66.  
763 <https://doi.org/10.1111/mec.14053>.

764 Cullen, Paul J., and George F. Sprague. 2012. “The Regulation of Filamentous Growth in Yeast.”  
765 *Genetics* 190 (1): 23–49. <https://doi.org/10.1534/genetics.111.127456>.

766 David-Vaizant, Vanessa, and Hervé Alexandre. 2018. “Flor Yeast Diversity and Dynamics in  
767 Biologically Aged Wines.” *Frontiers in Microbiology* 9 (SEP): 1–16.  
768 <https://doi.org/10.3389/fmicb.2018.02235>.

769 Delcourt, F., P. Taillandier, F. Vidal, and P. Strehaiano. 1995. “Influence of PH, Malic Acid and  
770 Glucose Concentrations on Malic Acid Consumption by *Saccharomyces Cerevisiae*.”  
771 *Applied Microbiology and Biotechnology* 43 (2): 321–24.  
772 <https://doi.org/10.1007/BF00172832>.

773 Eder, Matthias, Isabelle Sanchez, Claire Brice, Carole Camarasa, Jean Luc Legras, and Sylvie  
774 Dequin. 2018. “QTL Mapping of Volatile Compound Production in *Saccharomyces*  
775 *Cerevisiae* during Alcoholic Fermentation.” *BMC Genomics* 19 (1).  
776 <https://doi.org/10.1186/s12864-018-4562-8>.

777 Effelsberg, Daniel, Luis Daniel Cruz-Zaragoza, Jason Tonillo, Wolfgang Schliebs, and Ralf  
778 Erdmann. 2015. “Role of Pex 21p for Piggyback Import of Gpd1p and Pnc1p into  
779 Peroxisomes of *Saccharomyces Cerevisiae*.” *Journal of Biological Chemistry* 290 (42):  
780 25333–42. <https://doi.org/10.1074/jbc.M115.653451>.

781 Ehsani, Maryam, Maria R. Fernández, Josep a. Biosca, and Sylvie Dequin. 2009. “Reversal of  
782 Coenzyme Specificity of 2,3-Butanediol Dehydrogenase from *Saccharomyces Cerevisiae*  
783 and in Vivo Functional Analysis.” *Biotechnology and Bioengineering* 104 (2): 381–89.



784 <https://doi.org/10.1002/bit.22391>.

785 Fidalgo, Manuel, Ramon R. Barrales, Jose I. Ibeas, and Juan Jimenez. 2006. "Adaptive Evolution  
786 by Mutations in the FLO11 Gene." *Proceedings of the National Academy of Sciences of*  
787 *the United States of America* 103 (30): 11228–33.  
788 <https://doi.org/10.1073/pnas.0601713103>.

789 Fournier, T., O. Abou Saada, J. Hou, J. Peter, E. Caudal, and J. Schacherer. 2019. "Extensive  
790 Impact of Low-Frequency Variants on the Phenotypic Landscape at Population-Scale."  
791 *ELife* 8 (October). <https://doi.org/10.7554/eLife.49258>.

792 Ghislain, Michel, Emmanuel Talla, and Jean M. François. 2002. "Identification and Functional  
793 Analysis of the *Saccharomyces Cerevisiae* Nicotinamidase Gene, *PNC1*." *Yeast* 19 (3):  
794 215–24. <https://doi.org/10.1002/yea.810>.

795 Giannakou, Konstantina, Mark Cotterrell, and Daniela Delneri. 2020. "Genomic Adaptation of  
796 *Saccharomyces* Species to Industrial Environments." *Frontiers in Genetics* 11 (August):  
797 916. <https://doi.org/10.3389/fgene.2020.00916>.

798 Gladieux, Pierre, Jeanne Ropars, H el ene Badouin, Antoine Branca, Gabriela Aguilera, Damien  
799 M. De Vienne, Ricardo C. Rodr iguez De La Vega, Sara Branco, and Tatiana Giraud. 2014.  
800 "Fungal Evolutionary Genomics Provides Insight into the Mechanisms of Adaptive  
801 Divergence in Eukaryotes." *Molecular Ecology* 23 (4): 753–73.  
802 <https://doi.org/10.1111/mec.12631>.

803 Haley, C. S., and S. A. Knott. 1992. "A Simple Regression Method for Mapping Quantitative  
804 Trait Loci in Line Crosses Using Flanking Markers." *Heredity* 69 (4): 315–24.  
805 <https://doi.org/10.1038/hdy.1992.131>.

806 Hohmann, Stefan. 2009. "Control of High Osmolarity Signalling in the Yeast *Saccharomyces*  
807 *Cerevisiae*." *FEBS Letters* 583 (24): 4025–29.  
808 <https://doi.org/10.1016/j.febslet.2009.10.069>.

809 Huet, Carine, Javier Menendez, Carlos Gancedo, and Jean M. François. 2000. "Regulation of  
810 *Pyc1* Encoding Pyruvate Carboxylase Isozyme I by Nitrogen Sources in *Saccharomyces*

811 Cerevisiae.” *European Journal of Biochemistry* 267 (23): 6817–23.  
812 <https://doi.org/10.1046/j.1432-1033.2000.01779.x>.

813 Klein, C., L. Olsson, and J. Nielsen. 1998. “Glucose Control in *Saccharomyces Cerevisiae* : The  
814 Role of M/G7 in Metabolic Functions.” *Microbiology* 144: 13–24.

815 Kontoudakis, Nikolaos, Mireia Esteruelas, Francesca Fort, Joan Miquel Canals, Victor De  
816 Freitas, and Fernando Zamora. 2011. “Influence of the Heterogeneity of Grape Phenolic  
817 Maturity on Wine Composition and Quality.” *Food Chemistry* 124 (3): 767–74.  
818 <https://doi.org/10.1016/J.FOODCHEM.2010.06.093>.

819 Kubo, Yoshito, Hiroshi Takagi, and Shigeru Nakamori. 2000. “Effect of Gene Disruption of  
820 Succinate Dehydrogenase on Succinate Production in a Sake Yeast Strain.” *Journal of  
821 Bioscience and Bioengineering* 90 (6): 619–24. [https://doi.org/10.1016/S1389-  
822 1723\(00\)90006-9](https://doi.org/10.1016/S1389-1723(00)90006-9).

823 Kutyna, D. R., C. Varela, G. a. Stanley, a. R. Borneman, P. a. Henschke, and P. J. Chambers.  
824 2012. “Adaptive Evolution of *Saccharomyces Cerevisiae* to Generate Strains with  
825 Enhanced Glycerol Production.” *Applied Microbiology and Biotechnology* 93 (3): 1175–  
826 84. <https://doi.org/10.1007/s00253-011-3622-7>.

827 Kutyna, Dariusz R., Cristian Varela, Paul a. Henschke, Paul J. Chambers, and Grant a. Stanley.  
828 2010. “Microbiological Approaches to Lowering Ethanol Concentration in Wine.” *Trends  
829 in Food Science and Technology* 21 (6): 293–302.  
830 <https://doi.org/10.1016/j.tifs.2010.03.004>.

831 Kwast, K E, P V Burke, and R O Poyton. 1998. “Oxygen Sensing and the Transcriptional  
832 Regulation of Oxygen-Responsive Genes in Yeast.” *Journal of Experimental Biology* 201  
833 (8).

834 Leeuwen, Cornelis van, and Philippe Darriet. 2016. “The Impact of Climate Change on  
835 Viticulture and Wine Quality.” *Journal of Wine Economics* 11 (1): 150–67.  
836 <https://doi.org/DOI: 10.1017/jwe.2015.21>.

837 Legras, Jean-luc, Jaime Moreno-garcia, Severino Zara, Giacomo Zara, Teresa Garcia-martinez,

- 838 Juan C Mauricio, Ilaria Mannazzu, et al. 2016. "Flor Yeast : New Perspectives Beyond  
839 Wine Aging" 7 (April): 1–11. <https://doi.org/10.3389/fmicb.2016.00503>.
- 840 Legras, Jean Luc, Virginie Galeote, Frederic Bigey, Carole Camarasa, Souhir Marsit, Thibault  
841 Nidelet, Isabelle Sanchez, et al. 2018. "Adaptation of *s. Cerevisiae* to Fermented Food  
842 Environments Reveals Remarkable Genome Plasticity and the Footprints of  
843 Domestication." *Molecular Biology and Evolution* 35 (7): 1712–27.  
844 <https://doi.org/10.1093/molbev/msy066>.
- 845 Marsit, S., A. Mena, F. Bigey, F.-X. Sauvage, A. Couloux, J. Guy, J.-L. Legras, E. Barrio, S. Dequin,  
846 and V. Galeote. 2015. "Evolutionary Advantage Conferred by an Eukaryote-to-Eukaryote  
847 Gene Transfer Event in Wine Yeasts." *Molecular Biology and Evolution*, March, msv057-  
848 <https://doi.org/10.1093/molbev/msv057>.
- 849 Martí-Raga, Maria, Emilien Peltier, Albert Mas, Gemma Beltran, and Philippe Marullo. 2017.  
850 "Genetic Causes of Phenotypic Adaptation to the Second Fermentation of Sparkling  
851 Wines in *Saccharomyces Cerevisiae*." *G3: Genes, Genomes, Genetics* 7 (2): 399–412.  
852 <https://doi.org/10.1534/g3.116.037283>.
- 853 Marullo, Philippe, Telma da Silva, Warren Albertin, Mélisande Blein-Nicolas, Christine  
854 Dillmann, Marina Bely, Stéphane la Guerche, et al. 2015. "Hybridization within  
855 *Saccharomyces* Genus Results in Homeostasis, Heterosis and Phenotypic Novelty in  
856 Winemaking Conditions." In *10e Édition Du Symposium International d 'Œnologie*  
857 *Bordeaux*. Bordeaux: Dunod.
- 858 McCouch, Susan. 2004. "Diversifying Selection in Plant Breeding." *PLoS Biology*. Public Library  
859 of Science. <https://doi.org/10.1371/journal.pbio.0020347>.
- 860 Mira de Orduña, Ramón. 2010. "Climate Change Associated Effects on Grape and Wine Quality  
861 and Production." *Food Research International* 43 (7): 1844–55.  
862 <https://doi.org/10.1016/J.FOODRES.2010.05.001>.
- 863 Moreno-García, Jaime, Teresa García-Martínez, M. Carmen Millán, Juan Carlos Mauricio, and  
864 Juan Moreno. 2015. "Proteins Involved in Wine Aroma Compounds Metabolism by a  
865 *Saccharomyces Cerevisiae* Flor-Velum Yeast Strain Grown in Two Conditions." *Food*

866 *Microbiology* 51: 1–9. <https://doi.org/10.1016/j.fm.2015.04.005>.

867 Moreno-García, Jaime, Teresa García-Martínez, Juan Moreno, and Juan Carlos Mauricio. 2015.  
868 “Proteins Involved in Flor Yeast Carbon Metabolism under Biofilm Formation Conditions.”  
869 *Food Microbiology* 46: 25–33. <https://doi.org/https://doi.org/10.1016/j.fm.2014.07.001>.

870 Nevoigt, Elke, and Ulf Stahl. 1997. “Osmoregulation and Glycerol Metabolism in the Yeast  
871 *Saccharomyces Cerevisiae*.” *FEMS Microbiology Reviews* 21 (3): 231–41.  
872 [https://doi.org/10.1016/S0168-6445\(97\)00058-2](https://doi.org/10.1016/S0168-6445(97)00058-2).

873 Novo, Maite, Frédéric Bigey, Emmanuelle Beyne, Virginie Galeote, Frédérick Gavory, Sandrine  
874 Mallet, Brigitte Cambon, et al. 2009. “Eukaryote-to-Eukaryote Gene Transfer Events  
875 Revealed by the Genome Sequence of the Wine Yeast *Saccharomyces Cerevisiae*  
876 EC1118.” *Proceedings of the National Academy of Sciences of the United States of*  
877 *America* 106 (38): 16333–38. <https://doi.org/10.1073/pnas.0904673106>.

878 Olson-Manning, Carrie F., Maggie R. Wagner, and Thomas Mitchell-Olds. 2012. “Adaptive  
879 Evolution: Evaluating Empirical Support for Theoretical Predictions.” *Nature Reviews*  
880 *Genetics*. Nature Publishing Group. <https://doi.org/10.1038/nrg3322>.

881 Peltier, E, Vikas Sharma, M Marti Raga, M Roncoroni, M Bernard, V Jiranek, Y Gibon, and  
882 Philippe Marullo. 2018. “Genetic Basis of Genetic x Environment Interaction in an  
883 Enological Context.” *BMC Genomics*.

884 Peltier, Emilien, Margaux Bernard, Marine Trujillo, Duyên Prodhomme, Jean Christophe Barbe,  
885 Yves Gibon, and Philippe Marullo. 2018. “Wine Yeast Phenomics: A Standardized  
886 Fermentation Method for Assessing Quantitative Traits of *Saccharomyces Cerevisiae*  
887 Strains in Enological Conditions.” Edited by Joseph Schacherer. *PLoS ONE* 13 (1):  
888 e0190094. <https://doi.org/10.1371/journal.pone.0190094>.

889 Peltier, Emilien, Anne Friedrich, Joseph Schacherer, and Philippe Marullo. 2019. “Quantitative  
890 Trait Nucleotides Impacting the Technological Performances of Industrial *Saccharomyces*  
891 *Cerevisiae* Strains.” *Frontiers in Genetics* 10 (July): 683.  
892 <https://doi.org/10.3389/fgene.2019.00683>.

893 Peltier, Emilien, Vikas Sharma, Maria Martí Raga, Miguel Roncoroni, Margaux Bernard, Yves  
894 Gibon, Philippe Marullo, Vladimir Jiranek, Yves Gibon, and Philippe Marullo. 2018.  
895 “Dissection of the Molecular Bases of Genotype x Environment Interactions: A Study of  
896 Phenotypic Plasticity of *Saccharomyces Cerevisiae* in Grape Juices.” *BMC Genomics* 19:  
897 772. <https://doi.org/10.1186/s12864-018-5145-4>.

898 Pérez-Ortín, José E., Amparo Querol, Sergi Puig, and Eladio Barrio. 2002. “Molecular  
899 Characterization of a Chromosomal Rearrangement Involved in the Adaptive Evolution of  
900 Yeast Strains.” *Genome Research* 12 (10): 1533–39. <https://doi.org/10.1101/gr.436602>.

901 Peter, Jackson, Matteo De Chiara, Anne Friedrich, Jia Xing Yue, David Pflieger, Anders  
902 Bergström, Anastasie Sigwalt, et al. 2018. “Genome Evolution across 1,011  
903 *Saccharomyces Cerevisiae* Isolates.” *Nature* 556 (7701): 339–44.  
904 <https://doi.org/10.1038/s41586-018-0030-5>.

905 Pitoniak, Andrew, Barbara Birkaya, Heather M. Dionne, Nadia Vadaie, and Paul J. Cullen. 2009.  
906 “The Signaling Mucins Msb2 and Hkr1 Differentially Regulate the Filamentation Mitogen-  
907 Activated Protein Kinase Pathway and Contribute to a Multimodal Response.” *Molecular*  
908 *Biology of the Cell* 20: 3101–14. <https://doi.org/10.1091/mbc.E08>.

909 Pronk, Jack T., H. Yde Steensma, and Johannes P. Van Dijken. 1996. “Pyruvate Metabolism in  
910 *Saccharomyces Cerevisiae*.” *Yeast*. John Wiley & Sons, Ltd.  
911 [https://doi.org/10.1002/\(SICI\)1097-0061\(199612\)12:16<1607::AID-YEA70>3.0.CO;2-4](https://doi.org/10.1002/(SICI)1097-0061(199612)12:16<1607::AID-YEA70>3.0.CO;2-4).

912 R Core Team. 2018. “R: A Language and Environment for Statistical Computing.” *R Foundation*  
913 *for Statistical Computing, Vienna, Austria*. URL <https://www.R-project.org/>.

914 Ross-Ibarra, Jeffrey, Peter L. Morrell, and Brandon S. Gaut. 2007. “Plant Domestication, a  
915 Unique Opportunity to Identify the Genetic Basis of Adaptation.” *Proceedings of the*  
916 *National Academy of Sciences of the United States of America* 104 (SUPPL. 1): 8641–48.  
917 <https://doi.org/10.1073/pnas.0700643104>.

918 Rossouw, D, E H Heyns, M E Setati, S Bosch, and F F Bauer. 2013. “Adjustment of Trehalose  
919 Metabolism in Wine *Saccharomyces Cerevisiae* Strains to Modify Ethanol Yields.” *Applied*  
920 *and Environmental Microbiology* 79 (17): 5197–5207.

- 921 <https://doi.org/10.1128/AEM.00964-13>.
- 922 Saayman, M., and M. Viljoen-Bloom. 2017. "The Biochemistry of Malic Acid Metabolism by  
923 Wine Yeasts – A Review." *South African Journal of Enology & Viticulture* 27 (2).  
924 <https://doi.org/10.21548/27-2-1612>.
- 925 Salmon, Jean-michel. 1987. "L-Malic-Acid Permeation in Resting Cells of Anaerobically Grown  
926 *Saccharomyces Cerevisiae*." *Biochimica et Biophysica Acta (BBA) - Biomembranes* 901 (1):  
927 30–34. [https://doi.org/10.1016/0005-2736\(87\)90253-7](https://doi.org/10.1016/0005-2736(87)90253-7).
- 928 Sherman, Rachel M., and Steven L. Salzberg. 2020. "Pan-Genomics in the Human Genome  
929 Era." *Nature Reviews Genetics*, February, 1–12. [https://doi.org/10.1038/s41576-020-](https://doi.org/10.1038/s41576-020-0210-7)  
930 0210-7.
- 931 Sicard, Delphine, and Jean Luc Legras. 2011. "Bread, Beer and Wine: Yeast Domestication in  
932 the *Saccharomyces Sensu Stricto* Complex." *Comptes Rendus - Biologies*. Elsevier Masson  
933 SAS. <https://doi.org/10.1016/j.crv.2010.12.016>.
- 934 Silva, Telma da, Warren Albertin, Christine Dillmann, Marina Bely, Stéphane la Guerche,  
935 Christophe Giraud, Sylvie Huet, et al. 2015. "Hybridization within *Saccharomyces* Genus  
936 Results in Homeostasis and Phenotypic Novelty in Winemaking Conditions." Edited by  
937 Joseph Schacherer. *PLOS ONE* 10 (5): e0123834.  
938 <https://doi.org/10.1371/journal.pone.0123834>.
- 939 Steinmetz, Lars M., Himanshu Sinha, Dan R. Richards, Jamie I. Spiegelman, Peter J. Oefner,  
940 John H. McCusker, and Ronald W. Davis. 2002. "Dissecting the Architecture of a  
941 Quantitative Trait Locus in Yeast." *Nature*. Nature Publishing Group.  
942 <https://doi.org/10.1038/416326a>.
- 943 Stucka, Rolf, Sylvie Dequin, Jean Michel Salmon, and Carlos Gancedo. 1991. "DNA Sequences  
944 in Chromosomes 11 and VII Code for Pyruvate Carboxylase Isoenzymes in *Saccharomyces*  
945 *Cerevisiae*: Analysis of Pyruvate Carboxylase-Deficient Strains." *MGG Molecular &*  
946 *General Genetics* 229 (2): 307–15. <https://doi.org/10.1007/BF00272171>.
- 947 Szklarczyk, Damian, Annika L Gable, David Lyon, Alexander Junge, Stefan Wyder, Jaime Huerta-

- 948 Cepas, Milan Simonovic, et al. 2019. "STRING V11: Protein-Protein Association Networks  
949 with Increased Coverage, Supporting Functional Discovery in Genome-Wide  
950 Experimental Datasets." *Nucleic Acids Research* 47 (D1): D607–13.  
951 <https://doi.org/10.1093/nar/gky1131>.
- 952 Tatebayashi, Kazuo, Keiichiro Tanaka, Hui-Yu Yang, Katsuyoshi Yamamoto, Yusaku Matsushita,  
953 Taichiro Tomida, Midori Imai, and Haruo Saito. 2007. "Transmembrane Mucins Hkr1 and  
954 Msb2 Are Putative Osmosensors in the SHO1 Branch of Yeast HOG Pathway." *The EMBO*  
955 *Journal* 26 (15): 3521–33. <https://doi.org/10.1038/sj.emboj.7601796>.
- 956 Tilloy, Valentin, Axelle Cadière, Maryam Ehsani, and Sylvie Dequin. 2015. "Reducing Alcohol  
957 Levels in Wines through Rational and Evolutionary Engineering of *Saccharomyces*  
958 *Cerevisiae*." *International Journal of Food Microbiology* 213: 49–58.  
959 <https://doi.org/10.1016/j.ijfoodmicro.2015.06.027>.
- 960 Tilloy, Valentin, Anne Ortiz-Julien, and Sylvie Dequin. 2014. "Reduction of Ethanol Yield and  
961 Improvement of Glycerol Formation by Adaptive Evolution of the Wine Yeast  
962 *Saccharomyces Cerevisiae* under Hyperosmotic Conditions." *Applied and Environmental*  
963 *Microbiology* 80 (8): 2623–32. <https://doi.org/10.1128/AEM.03710-13>.
- 964 Volschenk, H., H. J.J. van Vuuren, and M. Viljoen-Bloom. 2003. "Malo-Ethanolic Fermentation  
965 in *Saccharomyces* and *Schizosaccharomyces*." *Current Genetics*.  
966 <https://doi.org/10.1007/s00294-003-0411-6>.
- 967 Walker, Michelle E., Dale L. Val, Manfred Rohde, Rodney J. Devenish, and John C. Wallace.  
968 1991. "Yeast Pyruvate Carboxylase: Identification of Two Genes Encoding Isoenzymes."  
969 *Biochemical and Biophysical Research Communications* 176 (3): 1210–17.  
970 [https://doi.org/10.1016/0006-291X\(91\)90414-3](https://doi.org/10.1016/0006-291X(91)90414-3).
- 971 Will, Jessica L., Hyun Seok Kim, Jessica Clarke, John C. Painter, Justin C. Fay, and Audrey P.  
972 Gasch. 2010. "Incipient Balancing Selection through Adaptive Loss of Aquaporins in  
973 Natural *Saccharomyces Cerevisiae* Populations." Edited by Leonid Kruglyak. *PLoS Genet* 6  
974 (4): e1000893. <https://doi.org/10.1371/journal.pgen.1000893>.
- 975 Zimmer, Adrien, Cécile Durand, Nicolás Loira, Pascal Durrens, David James Sherman, and

976 Philippe Marullo. 2014. "QTL Dissection of Lag Phase in Wine Fermentation Reveals a  
977 New Translocation Responsible for *Saccharomyces Cerevisiae* Adaptation to Sulfite."  
978 *PLoS ONE* 9 (1). <https://doi.org/10.1371/journal.pone.0086298>.

979